Elsevier Editorial System(tm) for Quaternary Science Reviews

Manuscript Draft

Manuscript Number: JQSR-D-16-00135R3

Title: The linking of the upper-middle and lower reaches of the Yellow River as a result of fluvial entrenchment

Article Type: SI:Fluvial Archives Group

Keywords: Yellow River; Sanmen gorge; Fenwei graben; Terrace; Planation surface; Fluvial incision rate

Corresponding Author: Dr. Zhenbo Hu, Ph.D.

Corresponding Author's Institution: Lanzhou University

First Author: Zhenbo Hu, Ph.D.

Order of Authors: Zhenbo Hu, Ph.D.; Baotian Pan, Ph.D.; David R Bridgland, Ph.D.; Jef Vandenberghe, Ph.D.; Lianyong Guo, Master; Yunlong Fan, Ph.D.; Rob Westaway, Ph.D.

Abstract: The upper-middle Yellow River flows through the Fenwei graben, a structure resulting from extensional tectonism that was formed and repeatedly extended during the Cenozoic. The drainage system within this graben was formerly isolated from the lower reaches of the Yellow River system by the Xiaoshan mountains, an actively growing ~NW-SE trending range. The modern course of the Yellow River takes it through this range along the Sanmen gorge, the formation of which was of great significance in that it initiated through-going drainage between the upper-middle and lower reaches of the system. The timing of this event, which was clearly a criticial point in the evolution of the Yellow River, can be established by dating the terraces in the gorge. Intermittent deepening of this gorge by the Yellow River from a high-level planation surface capping the mountain range has resulted in the formation of five terraces. Magnetostratigraphic records from aeolian deposits accumulated on these surfaces provide a geochronological sequence for this geomorphic archive, in which the ages of the planation surface and of terraces T5, T4, T3, T2, and T1 have been determined as ~3.63 Ma, ~1.24 Ma, ~0.86 Ma, ~0.62 Ma, ~129 ka, and ~12 ka, respectively.
Under the constraint of this chronological framework, a model for landscape evolution is proposed here. Uplift of the inner Fenwei graben and of the surrounding mountain ranges led to dissection of the 3.63 Ma old planation surface in conjunction with the formation of the Sanmen gorge. Drainage of the lake previously occupying the basin would have promoted incision into the fluvio-lacustrine graben sediments; indeed, gorge formation through the Xiaoshan may have been initiated or intensified by lake overflow. The ages obtained for the planation surface and uppermost terrace suggest that the formation of the Sanmen gorge and the initiation of the through-going eastward drainage of the Yellow River occurred between 3.63 and 1.24 Ma. Before the start of gorge entrenchment, the products of erosion in the modern upper catchment of the Yellow River were unable to reach the sea. The dramatic increase in deposition rates in the Bohai Gulf (at the mouth of the modern Yellow River in the East China Sea), ~1.0 Ma ago, thus resulted from the

initiation of an integral (enlarged) Yellow River catchment drainage through the Sanmen gorge; it does not imply an increase in erosion rates at that time.

Dear Editor,

re: revised manuscript with reference number ‘JQSR-D-16-00135R2’.
Title: The linking of the upper-middle and lower reaches of the Yellow River as a result of fluvial entrenchment
Authors: Zhenbo Hu*, Baotian Pan, David Bridgland, Jef Vandenberghe, Lianyong Guo, Yunlong Fan, Rob Westaway

Please, find enclosed our revised manuscript intended for publication in the FLAG special issue of “Quaternary Science Reviews”.

It should be pointed out that this work is a thorough improved version of our previous manuscript.

The referee and guest editor stated many valuable comments and constructive suggestions. According to these comments and suggestions, we made a point to point revision to the previous manuscript, with an item-by-item explanation attached.

We like to express our great appreciation for your editorial efforts.

With our best regards,
Zhenbo Hu
Corresponding author of JQSR-D-16-00135R2

The linking of the upper-middle and lower reaches of the Yellow River as a result of fluvial entrenchment

ZhenBo Hu[a,] *, BaoTian Pan[a,] *, David Bridgland[b], Jef Vandenberghe[c], LianYong Guo[a], YunLong Fan[a], Rob Westaway[d]

[a]Key Laboratory of Western China's Environmental Systems (Ministry of Education), College of Earth and Environmental Sciences, Lanzhou University, Lanzhou 730000, People's Republic of China

[b]Department of Geography, Durham University, South Road, Durham DH1 3LE, UK

[c]Department of Earth Sciences, Vrije Universiteit, De Boelelaan 1085, 1081 HV Amsterdam, The Netherlands

[d]School of Engineering, University of Glasgow, James Watt (South) Building, Glasgow G12 8QQ, UK

*Corresponding author. E-mail: zhbhu@lzu.edu.cn; hu_zhb@126.com (Z. Hu)

Abstract

The upper–middle Yellow River flows through the Fenwei graben, a structure resulting from extensional tectonism that was formed and repeatedly extended during the Cenozoic. The drainage system within this graben was formerly isolated from the lower reaches of the Yellow River system by the Xiaoshan mountains, an actively growing ~NW–SE trending range. The modern course of the Yellow River takes it through this range along the Sanmen gorge, the formation of which was of great significance in that it initiated through-going drainage between the upper–middle and lower reaches of the system. The timing of this event, which was clearly a criticial point in the evolution of the Yellow River, can be established by dating the terraces in the gorge. Intermittent deepening of this gorge by the Yellow River from a high-level planation surface capping the mountain range has resulted in the formation of five terraces. Magnetostratigraphic records from aeolian deposits accumulated on these surfaces provide a geochronological sequence for this geomorphic archive, in which the ages of the planation surface and of terraces T5, T4, T3, T2, and T1 have been determined as ~3.63 Ma, ~1.24 Ma, ~0.86 Ma, ~0.62 Ma, ~129 ka, and ~12 ka, respectively.

Under the constraint of this chronological framework, a model for landscape evolution is proposed here. Uplift of the inner Fenwei graben and of the surrounding mountain ranges led to dissection of the 3.63 Ma old planation surface in conjunction with the formation of the Sanmen gorge. Drainage of the lake previously occupying the basin would have promoted incision into the fluvio-lacustrine graben sediments; indeed, gorge formation through the Xiaoshan may have been initiated or intensified by lake overflow. The ages obtained for the planation surface and uppermost terrace suggest that the formation of the Sanmen gorge and the initiation of the through-going eastward drainage of the Yellow River occurred between 3.63 and 1.24 Ma. Before the start of gorge entrenchment, the products of erosion in the modern upper catchment of the Yellow River were unable to reach the sea. The dramatic increase in deposition rates in the Bohai Gulf (at the mouth of the modern Yellow River in the East China Sea), ~1.0 Ma ago, thus resulted from the initiation of an integral (enlarged) Yellow River catchment drainage through the Sanmen gorge; it does not imply an increase in erosion rates at that time.

*Keywords***:** Yellow River; Sanmen gorge; Fenwei graben; Terrace; Planation surface; Fluvial incision rate

1. Introduction

Many of the world's largest rivers flow along structural lows and major rift systems (Potter, 1978) and, meanwhile, have shaped the landscape over large areas. In those regions that have been entrenched, the interaction between climate, uplift, lithology, and base level have been fundamental controls on the evolution of fluvial systems (Schumm et al., 2000; Veldkamp and van Dijke, 2000; Pan et al., 2003; Bridgland and Westaway, 2008; Vandenberghe et al., 2011). Moreover, information about tectonic activity and climatic change can be imprinted into sedimentary and morphological fluvial archives (e.g., Bridgland, 2000; Stokes, 2008; Westaway, 2009; Craddock et al., 2010; Bridgland et al., 2012; Bridgland and Westaway, 2014). The development of large rivers is thus widely employed to determine the history of structural, environmental, and topographical change during the Quaternary.

The formation of the Tibetan Plateau is generally thought to have been an amplifier and driver for the environmental evolution of East Asia, strengthening the East Asian monsoon and thus having an influence on precipitation and related erosion rates (Li, 1991; Pan et al., 1995; Liu and Chen, 2000). Constraint on its uplift history provides the basis for understanding the effects of high topography on climate and on various earth surface processes (An et al., 2001).

The development of fluvial systems in East Asia has also been closely associated with topographical evolution since the India–Eurasia collision (e.g., Powell and Conaghan, 1973; Lin et al., 2001; Fan and Li, 2008). The eastward flow direction of the largest rivers in China (e.g., the Yellow River and the Yangtze) is generally attributed to the relative eastward decline of the macro-relief, resulting from the uplift of the Tibetan Plateau (Miao et al., 2008; Craddock et al., 2010; Zheng et al., 2013). Marine accumulation of terrigenous sediments derived from these large fluvial systems may be assumed to have started in the Bohai Gulf immediately after the formation of this drainage pattern (Zheng et al., 2004; Jiang et al., 2007). The establishment of these eastward-flowing drainage systems provides a critical link between upland erosion and the marine accumulation of terrigenous sediments (Nie et al., 2015). Despite much attention having been paid to long-term fluvial landscape development in East Asia, which is related to the uplift of the Tibetan Plateau during the Quaternary, the formation age of the eastward drainage pattern in China is still strongly debated (cf. Lin et al., 2001; Clark et al., 2004; Pan et al., 2005b; Clift, 2006;

Zheng et al., 2007, 2013). It is the specific objective of this paper to reconstruct the eastward drainage history of the Yellow River by dating its terraces in the critical reach between its middle and lower catchments. The formation ages of terraces T4, T3 and T2 at Sanmenxia were determined previously by Pan et al. (2005a) as 0.86 Ma, 0.62 Ma, and 0.129 Ma, respectively, but no dating was available for the highest terrace T5 and the planation level in the study region.

2. Regional geological and geomorphic setting

2.1. General position of the Ordos block, Fenwei graben and Xiaoshan mountains

The Ordos block is an upland massif located at the northeastern margin of the Tibetan Plateau and bounded by graben systems. During the Mesozoic, this block was a large basin with an area of ~320,000 km^2 (Zhu et al., 2008) and was filled with terrigenous clastic sediments. Following the Indo-Asian collision (Molnar et al., 1993), deformation progressively propagated from the collision zone to the northeastern margin of the Tibetan Plateau (Tapponnier et al., 2001; Fig. 1, inset). Arc-shaped thrust faults and strike-slip fault systems were thus generated between the Ordos block and the Tibetan Plateau, leading to the formation, by extensional stress, of the crescent-shaped Fenwei graben (Zhang et al., 1998, 2003; Huang et al., 2008; Liu et al., 2013). Meanwhile, the Ordos block and the Qinling, Huashan, Luliang, and Taihang (including the Xiaoshan) mountains were uplifted with respect to this subsiding graben (AFSOM, 1988). In the middle reaches of the Yellow River, the landscape is characterized by a topography of alternating depressions and rolling uplands, consisting of the above-mentioned ranges. Apatite fission track data and geomorphic chronology have indicated that this area was uplifted in the early Miocene and was then planated by the late Neogene (Yuan et al., 2007; Pan et al., 2012).

<Fig. 1 hereabout>

The Fenwei graben is a NE–SW trending, crescent-shaped subsided area constrained by numerous normal and strike-slip faults, covering more than 20,000 km^2 (AFSOM, 1988; Fig. 1). Its basement is further intersected by internal

ENE-trending normal faults, forming four sub-basins, the Weihe, Fenhe, Yuncheng, and Lingbao basins (Fig. 1). The Fenwei graben is generally considered to have been an extensional area that was continuously subsiding during the Cenozoic, a response to the eastward extrusion of the Tibetan Plateau (Zhang et al., 1998, 2003); it has simultaneously been filled by ~4000 m of fluvio-lacustrine deposits (AFSOM, 1988). Based on previous investigation, these sediments dominate most of the graben, implying the existence of a large lake, from Sanmenxia in the east, Baoji in the west, the Qinling mountains in the south, and Yumenkou in the north (Liu, 2004; Fig. 1). These fluvio-lacustrine sediments are defined as the Sanmen Formation, characterized by undeformed, generally horizonal and parallel lithostratigraphy (AFSOM, 1988), pointing to regular vertical subsidence.

<Fig. 2 hereabout>

Subsidence, extensional tectonics and uplift have remained vigorous and active during the Quaternary in the area of the Fenwei graben. Fault scarps and triangular facets that can be traced for hundreds of kilometers are readily observed along the northern front of the Qinling, Huashan, and the southern front (Xiaoshan) of the Taihang Mountains (Dong et al., 2011). Major earthquakes around this graben are known from historical records (Zhang et al., 2003). The middle and lower reaches of the Yellow River are separated by the Xiaoshan mountains. To cross this topographic barrier the Yellow River has incised deeply into these mountains, creating the Sanmen gorge, between Sanmenxia and Xiaolangdi (Fig. 2 and Fig. 3). The Sanmen gorge is constrained by normal and strike-slip faults (Fig. 2), and is transected by numerous inferred inner faults (Fig. 3). Many ground fissures associated with earthquakes are exposed along these inferred faults within the gorge, indicating that uplift of the Xiaoshan with respect to the Lingbao basin, to the northwest, and the North China Plain (to the southeast) has never ceased (AFSOM, 1988).

<Fig. 3 hereabout>

The modern landscape in the vicinity of the Sanmen gorge is an uplifted and rolling surface that is well preserved on resistant rocks in the higher parts of the area. It represents a remnant of a planation surface that was cut through most of the

158 pre-existing tectonic structures and the relief right across the Lingbao basin, the
159 Xiaoshan range, and the North China Plain (Fig. 4A). This geomorphic surface was
160 deformed strongly over the Xiaoshan (Fig. 4B), forming a convexity between the
161 Lingbao basin and the North China Plain (Fig. 2). In general, its altitude exhibits a
162 declining trend towards the east, falling below 400 m in the North China Plain.
163
164 <Fig. 4 hereabout>
165
166 2.2. The downstream part of the Yellow River
167
168 The Yellow River (Huanghe) originating from the northeastern margin of the
169 Tibetan Plateau and flowing eastwards across China, crosses numerous tectonic zones
170 and major active faults. The Xiaoshan mountain range represents the final barrier to
171 be crossed by the river before it flows across the North China Plain and finally
172 debouches, attaining a total length of 5464 km (Wang et al., 2001), with its huge
173 sediment load, into the Bohai Gulf (Saito et al., 2001; Fig. 1, inset). The North China
174 Plain, which was formed from the steady supply of sediments from the upper and
175 middle reaches of the Yellow River, has remained close to sea level throughout the
176 Quaternary (Yang and Chen, 1985), experiencing marine inundation during some
177 interglacial periods (Geng, 1981). Sedimentary cores from this plain were analyzed in
178 an attempt to identify the oldest fluvial sediments from the Yellow River, thereby
179 dating the initiation of its eastward flow (Liu et al., 1988). However, the river has a
180 long history of wandering in disparate courses across the North China Plain, resulting
181 in deposition at different times at different sites, which has led to estimates for the
182 date of eastward-drainage initiation that range from Early to Late Pleistocene (Xia et
183 al., 1993; Yu, 1999; Wu et al., 2000; Yang et al., 2001).
184
185 2.3. The evolution of the Fenwei graben and the Sanmen gorge
186
187 The Fenwei graben, situated upstream of the Sanmen gorge, was occupied,
188 before the formation of the Yellow River, by a lake that covered the Weihe, Fenhe,
189 Yuncheng, and Lingbao basins (Liu, 2004). The ages of the uppermost
190 fluvio-lacustrine sediments within these basins range from 1.85 Ma to 150 ka (He et
191 al., 1984; Yue et al., 1999; Ji et al., 2006), representing an imprecise chronological

framework for the formation of the eastward drainage pattern of the Yellow River through the Sanmen gorge. Furthermore, recent work using cosmogenic nuclide dating, combined with provenance analysis of zircon and U–Pb age distributions, suggests that the Sanmen gorge was initially entrenched, during the period from 1.5 to 1.3 Ma, by the eastward draining Weihe River, which is now the largest tributary of the Yellow River (Kong et al., 2014). Comparative analysis of ostracod assemblages (Lishania) from the fluvio-lacustrine sediments in the Fenwei graben and from the fluvial sediments in the North China Plain suggests a close correlation between the two areas after ~1.0 Ma, implying the existence of eastward drainage by that time (Xue, 1996). Finally, at Mangshan, ~100 km downstream of the Sanmen gorge (Fig. 2), a dramatic increase in the accumulation rate of loess since the formation of palaeosol S2 was suggested to result from a proximal contribution of silt blown from the Yellow River floodplain, suggesting that eastward drainage had been formed at the latest by c. 243 ka, which is the formation age of S2 (Jiang et al., 2007; Zheng et al., 2007; Prins et al., 2009).

An important objective of this paper is to reconstruct the eastward drainage history of the Yellow River within a geochronological framework. The initiation of this eastward draining river has remained a highly controversial topic. Given that river terraces, as former floodplains (Bull, 1990; Merritt et al., 1994), can provide compelling evidence for determining drainage development (Stokes, 2008; Westaway et al., 2009; Vandenberghe et al., 2011), the dating of such terraces along the Sanmen gorge can provide important evidence (Pan et al., 2005a; Zheng et al., 2007; Kong et al., 2014). Most of the terraces in the gorge are directly overlain by thick aeolian loess covers, which can offer an excellent age control for the underlying terraces sediments (e.g., Liu, 1985; Pan et al., 2009, 2012; Guo et al., 2012). The chronological framework from these loess covers has been based on a combined approach of magnetostratigraphy, pedostratigraphy, electron spin resonance (ESR), and luminescence dating, and cosmogenic radionuclide geochronology (e.g., Cheng et al., 2002; Pan et al., 2009; Craddock et al., 2010; Zhang et al., 2010; Perrineau et al., 2011). From the constraint provided by the loess stratigraphy, the age of the highest Yellow River terrace at the downstream end of the Sanmen gorge was determined at 1.2 Ma by Pan et al. (2005b). In contrast, the oldest terrace at the gorge inlet was considered significantly younger, at only 0.8 Ma (Pan et al., 2005a). This temporal mismatch may be attributed to incomplete age control from the loess covers in the

gorge.

A series of well-preserved terraces was formed by the Yellow River in the Sanmen gorge during its incision into the Xiaoshan. Here, detailed field investigation was performed to establish a complete sequence of geomorphic surfaces. Next, a new geochronology for the geomorphic archive is presented, based on the combined approach of magnetostratigraphy, pedostratigraphy, and optically stimulated luminescence (OSL) dating of the aeolian cover on the geomorphic surfaces. Finally, this geochronology is used to constrain the formation age of the eastward-draining Yellow River.

<Fig. 5 hereabout>

3. Method

3.1. Field research

Intermittent downcutting by the Yellow River, starting from the planation surface and cutting into the bedrock of the Xiaoshan to form the Sanmen gorge, has given rise to a series of terraces along the valley. Field observations suggest that these terrace treads are generally disposed asymmetrically within the valley. To elucidate the formation history of the Yellow River within this gorge, work has focused on five geomorphic cross-sections, from Zhangbian to Kouma (Fig. 3). For each cross-section, terraces below the planation surface were identified and their tread heights (top of fluvial deposits) above river level determined, the characteristics of the fluvial deposits were described, and the thickness of overlying aeolian sediments (loess and Red Clay) was measured.

<Table 1 hereabout>

The five transect sites were selected as representative of the supposed relict planation surface and of the suite of lower-level fluvial terraces. The transect at Zhangbian is located within the Lingbao basin. The transects at Sanmenxia, Dongcun, and Xiaolangdi are located, respectively, at the inlet of, within, and at the outlet of the gorge, whereas the Kouma site is ~20 km downstream of the gorge (Fig. 3). Field

measurements of terrace elevation and the thickness of overlying aeolian cover were performed using a differential GPS system with an uncertainty of < 5 cm. According to these results, combined with loess stratigraphy and geomorphic surface tracking, terrace sequences at these sites were outlined (Fig. 5) and correlated (Table 1). It appears that the altitude of the planation surface and the vertical separation between high terrace treads and the present-day river level increase considerably at first and then gradually decrease with downstream distance along the gorge (Fig. 6). This topographical pattern corresponds with the convexity, mentioned above, thought to relate to the active uplift of the Xiaoshan range.

<Fig. 6 hereabout>

3.2. Aeolian deposits capping the geomorphic surfaces

The aeolian sediments (Tertiary Red Clay and overlying Quaternary loess) covering the planation surface and terrace treads provide valuable age estimates for the underlying landforms. However, the aeolian covers are rather thin at Dongcun and Xiaolangdi in comparison with those at Zhangbian, Sanmenxia, and Kouma, probably because accumulation was less in the confined Sanmen gorge (Fig. 5). Thus the Sanmenxia transect was selected for the analysis of magnetostratigraphy and pedostratigraphy of the aeolian sequence.

With reference to the established timescale of the aeolian sedimentary sequence on the Chinese Loess Plateau, enhanced by astronomical tuning and paleomagnetism, the basal ages of aeolian cover on each terrace along the Sanmen gorge can be determined. Readers are referred to Ding et al. (2002) for a detailed chronostratigraphic framework of the Chinese loess. Thus these aeolian series, in combination with their magnetostratigraphic and pedostratigraphic properties, provide a geochronological framework for the terrace sequences in the five Yellow River transects, as will now be described. The present study concentrates on the, hitherto undated, aeolian deposits above the planation surface and terrace T5.

3.3. Magnetic susceptibility measurements

Magnetic susceptibility reflects the layering of loess and palaeosols (Soreghan et

al., 1997) and thus can further confirm the identification of pedostratigraphic units and aid correlation. Powder samples were taken at 0.05-m intervals from the aeolian covers of the planation surface and uppermost terrace (T5). A total of 5650 samples were air-dried in the laboratory and then gently ground. Measurements with a Bartington MS2B magnetic susceptibility meter were used to obtain the mass magnetic susceptibility (Fig. 7).

<Fig. 7 hereabout>

3.4. Paleomagnetism

Samples were taken from the 152-m and 130.5-m thick aeolian deposits accumulated respectively on top of the planation surface and the uppermost terrace (T5). A total of 441 oriented block samples were collected at 0.25-m intervals in the Red Clay and at intervals of ~0.5–3.0 m in the loess. In the laboratory these samples were cut into 2-cm^3 transects, producing three sets of paleomagnetic logs. All the processed samples were thermally demagnetized in 15–17 steps at 50–30^oC intervals (between 50 and 680^oC) with an MMTD-80 Thermal Demagnetizer. Remanent magnetization and magnetic orientation were measured on a 2G-755R Superconductiing Rock Magnetometer in the magnetically shielded room of the Paleomagnetic Laboratory of the Key Laboratory of western China's Environmental System (MOE), Lanzhou University.

Two components are generally distinguished in the palaeomagnetic signal, by contrasting directions and intensities. A low-temperature component (LTC) in roughly the normal polarity direction is removed gradually by thermal treatment in the interval 100–150 ^oC (but sometimes up to 200–350 ^oC). This LTC is generally interpreted as a secondary remanent magnetization characterized by a viscous superimposed direction. Upon removal of the LTC, a high-temperature component (HTC) shows relatively stable directions and linear decay in intensity toward the origin. This HTC is generally interpreted as the primary magnetization acquired during deposition. The directions of the HTC are calculated using the least-squares fitting technique (Kirschvink, 1980) for selected demagnetization data points (minimum of three, but mostly 5–10).

4. Results

4.1. The terrace succession

A well-preserved sequence of five strath terraces was identified between the present river bed and the planation surface (Fig. 4C and D), within which the uppermost terrace is newly recognized in comparison with the previous study by Pan et al. (2005a). The term strath terrace is used here to describe an erosional terrace with only a relatively thin gravel layer, isolated vertically from the gravels of other terraces. In this terrace sequence, all treads are eroded into the Early Pleistocene lacustrine Sanmen Formation (see Fig. 4E for sedimentary characteristics). The planation surface, cut through pre-existing limestone, basin-fill sediments, and tectonic structures, is overlain by 12.5-m-thick Red Clay and a 139.5 m thick loess sequence, characterized by alternating loess (L) and palaeosol (S) units (Fig. 7). No indications of erosional disconformity between the Red Clay and the loess have been observed. Palaeosol complex S5, consisting of three sub-palaeosols, is the most prominent one within the sequence on the Chinese Loess Plateau, and is distinguished by its great thickness and dark color, being generally regarded as a marker layer (Liu, 1985). It can be discerned by field observations to occur at a depth of 107.6–115.3 m in the aeolian cover of the planation surface at Sanmenxia, which contains 32 palaeosol units (Fig. 7). The loess deposits above the gravels of terraces T5, T4, T3, and T2 are ~130, 114, 64, and 30 m thick respectively (Fig. 7). From detailed field observations, the loess stratigraphy on these four terraces can be divided, respectively, into fifteen, nine, six, and three red palaeosol units, which can be readily correlated with the upper palaeosol units (S14 to S1) on the planation surface. The basal palaeosol units of each terrace can be shown to overlie the fluvial deposits without a significant hiatus. In the case of the planation surface and terrace T5, these pedostratigraphic correlations, based on field observations, have been further corroborated by patterns of magnetic susceptibility variation (see below). The lowermost terrace has been OSL-dated to 12.7 ± 1.2 ka (HZB-2; Fig. 5).

4.2. Magnetic susceptibility

Magnetic susceptibility reflects the distinction between loess (L) and palaeosols (S), with higher values in palaeosols than in loess (e.g., Kukla et al., 1988; Maher and

Thompson, 1991; Soreghan et al., 1997). The variation patterns of magnetic susceptibility in the loess deposits on the planation surface and uppermost terrace (T5) are closely consistent with field observations of pedostratigraphy (Fig. 7). For palaeosol complex S5 in the two studied loess covers, the magnetic susceptibility increases steeply and reaches its highest value in the middle part of this complex, suggesting a prominently developed palaeosol unit. More specifically, large amplitude fluctuations of magnetic susceptibility appear in this palaeosol complex, showing three marked peaks that correspond well with the three subsidiary divisions of this prominent S5 palaeosol. Using S5 as a marker horizon, magnetic susceptibility data were used to divide the loess sequences on the planation surface and terrace T5, respectively, into 32 (from S1 to S32, with the basal loess unit L33) and 15 (Sm–S14) established palaeosol units. The magnetic susceptibility patterns from these two loess covers are in good agreement with comparable records from the Chinese Loess Plateau (e.g., Lu et al., 1999; Pan et al., 2012). Their high magnetic susceptibility values match well with the light red palaeosol units, implying that the pedostratigraphic divisions based on field observations, as described in this paper, are reliable.

The Red Clay beneath the Quaternary loess was deposited immediately on top of the planation surface. Its magnetic susceptibility gradually increases upwards, reaching its highest value at the top of the unit. Further upwards, the values decrease markedly in the overlying pedogenic carbonate nodule layer and then recover in the transitional layer (TU) between Red Clay and the overlying Quaternary loess. This pattern of magnetic susceptibility in the Red Clay obtained here concurs with magnetic susceptibility records from late Pliocene Red Clay sections on the Chinese Loess Plateau (Sun et al., 2006; Pan et al., 2011).

4.3. Paleomagnetism

Three sets of palaeomagnetic transects, collected from the aeolian covers of the planation surface and terrace T5 at each section, show similar properties. Most samples maintain strong remanent magnetization, with clear separation of characteristic remanent magnetization (ChRM) directions (see Fig. 8 for the typical thermal demagnetization diagrams).

<Fig. 8 hereabout>

The pedostratigraphy and magnetic patterns of the aeolian covers on the planation surface and uppermost terrace (T5) are illustrated in Fig. 7. The magnetostratigraphic patterns from the two covers can be correlated with the geomagnetic polarity timescale (GPTS) of Cande and Kent (1995).

In the 152.0-m thick aeolian deposits on the planation surface, both the stratigraphic subdivision of the loess and the conformity between the Red Clay and overlying loess deposits provide a reliable indication that the chronology of the aeolian cover extends from the Pliocene to the late Pleistocene (Liu, 1985). Thus the obtained magnetozones correlate typically with the polarity intervals from Brunhes to Gauss in the geomagnetic polarity timescale. The Gauss normal-polarity chron occurs between 0.5 and 11.5 m above the planation surface and includes two reversed-polarity subchrons that pinpoint the basal age of aeolian deposits here to the Kaena and Mammoth subchrons. The Gauss–Matuyama boundary occurs in the lower part of TU, which is also the boundary between the Neogene Red Clay and Quaternary loess (Liu, 1985; Ding et al., 1990). The Olduvai normal subchron, spanning 38–30 m, occurs between S27 and L25. The Jaramillo normal subchron, extending from 74.5 to 82.0 m, is registered between S11 and L10. The Matuyama-Brunhes boundary is found at a depth of 98.0 m in L8. These paleomagnetic polarity events identified in the stratigraphy on the planation surface are in full agreement with the well-established loess and Red Clay magnetostratigraphy on the Chinese Loess Plateau (cf. Kukla and An, 1989; Rutter et al., 1991; Zhu et al., 1994; Ding et al., 1998; Pan et al., 2012). On the Loess Plateau, since the sedimentation rate in the Red Clay (~1.5 cm/ky) was generally lower than that in the Quaternary loess (~10 cm/ky) (e.g., Vandenberghe et al., 2004), extrapolation of the prevailing accumulation rate of the Red Clay (here, ~1.1 cm/ky within the Gauss chron) below the lower boundary of the Gauss normal polarity chron is a more logical approach for dating the basal Red Clay, rather than using an accumulation rate averaged over the entire aeolian sequence (Red Clay and loess). This approach yields an estimated age of ~3.63 Ma for the onset of aeolian deposition on the planation suface.

For the ~130 m thick loess cover stacked on the uppermost terrace (T5), the Matuyama–Brunhes boundary occurs at a depth of 49.0 m and coincides with L8. The

Jaramillo normal subchron, spanning from 18.0 to 28.5 m, is registered between S11 and L10. It is clear that the positions of these paleomagnetic polarity events may readily be correlated with the magnetostratigraphy derived from the aeolian cover of the planation surface. Extrapolation of the prevailing accumulation rate of the loess deposits (~10.5 cm/ky) below the lower boundary of the Jaramillo normal subchron produces an estimated age of ~1.24 Ma for the basal loess deposits lying on this terrace.

5. Discussion

5.1. Age determination of the fluvial terraces within the Sanmen gorge

In most cases there is a gradual transition from terrace gravel to overbank sediments and, finally, to primary (in situ) aeolian deposits (Vandenberghe et al., 2012). Therefore, the basal age of the aeolian deposits immediately overlying the planation surface and terrace treads can be roughly equated with the formation times of the geomorphic surfaces (planation and fluvial terrace surfaces). Supplementary to the previous dating of terraces T4, T3, and T2 by Pan et al. (2005a), to 860, 620, and 129 ka, respectively, the newly recognized planation surface and uppermost terrace (T5) have now provided age estimates also (Fig. 7). Although the terrace called T5 here was previously recognized by Kong et al. (2014), its age was not determined successfully by their cosmogenic radio nuclide (CRN) study, which may be linked to the difficulty of getting reliable burial dates from river terrace deposits (Rixhon et al., 2016). In comparison, the latter authors assigned an age of 1.3 Ma to the lower sediments of terrace T4, which is older than the abandonment age of 860 ka obtained by Pan et al (2005a). According to the magnetostratigraphic analyses of the basal parts of the aeolian covers, the ages of the planation surface and terrace T5 are ~3.63 Ma and ~1.24 Ma, respectively; the latter age is close to the 1.5 – 1.3 Ma suggested by Kong et al. (2014) for the initiation of drainage (by the Weihe River) through the Sanmen gorge.

On the basis of field investigation, the tread of the uppermost terrace (T5) at Sanmenxia can be traced over an extensive area upstream and extending downstream into the inner Sanmen gorge, and can be correlated tentatively (based on height above modern river) with the uppermost terraces formed at Zhangbian, Dongcun, and

Xiaolangdi (Fig. 6). This distribution pattern indicates that the uppermost terrace below the planation surface is generally continuous, representing the initial fluvial incision by the Yellow River within the gorge. In addition, the magnetostratigraphic record from the uppermost terrace at Kouma, downstream of the Sanmen gorge, has also been dated previously to ~1.2 Ma (Pan et al., 2005b). The temporal coincidence of the uppermost terraces upstream and downstream of this gorge suggests that the first phase of downcutting by the Yellow River from the planation surface to the level of the uppermost terrace was prior to ~1.2 Ma (again in general agreement with the previous conclusions of Kong et al. (2014)).

5.2. Evolution of the middle to lower Yellow River catchment from basin filling to entrenchment

The magnetostratigraphic record from the aeolian cover of the planation surface at Sanmenxia suggests that before 3.63 Ma the Fenwei graben (represented by the Lingbao basin) had become progressively filled with the lacustrine sediments (Fig. 9AI). Geomorphic investigation along the Sanmen gorge (Fig. 5) indicates that at this time the local relief was progressively lowered to basin-fill level, eventually forming the planation surface (Fig. 9AII) that extends across the Fenwei graben and the surrounding mountain ranges (including the Xiaoshan) as was the case at the northern Tibetan Plateau (Wang et al., 2012).

<Fig. 9 hereabout>

Elsewhere, the development of low-relief landscapes (‘planation surface’) has been claimed as a reliable marker to indicate subsequent landscape rejuvenation, uplift and deformation (e.g., Ollier and Pain, 2000; Clark et al., 2004; Peulvast and Sales, 2004). Before and during the Pliocene, large parts of Europe, Africa, and Asia were planated, all in areas that were unaffected by plate motions, thus leading to the widespread development of low-relief landscapes (e.g., Cui et al., 1996; Danišík et al., 2006; Coltorti et al., 2007; Wagner et al., 2011; Pan et al., 2012; Vandenberghe, 2016). The comparable low-relief landscape or ‘planation surface’, recognized in and around the Fenwei graben and the Xiaoshan has been significantly uplifted by plate tectonic processes and subsequently dissected. The continuation of tectonic activity after the

formation of the planation level during the late Pliocene and Quaternary can be demonstrated. First, as is apparent from the geomorphic section at Sanmenxia (Fig. 5), the downthrow of the hanging-walls along the normal faults bounding the Lingbao basin (within the graben system of the Fenwei; Fig. 9B) disrupted the 'planation surface', which itself became uplifted in the Xiaoshan area. Second, seismic data also indicate that the normal faults bounding the Lingbao basin have remained active during the Quaternary (Li et al., 2015). The evolution of this active basin was probably independent of the rest of the southern Shanxi rift. As the Xiaoshan mountains grew higher, the ancestral fluvial system that drained their eastern front began to cut headward, toward the west (Wang et al., 2001).

The sedimentary record in the North Pacific indeed shows that dust deposition increased quite rapidly, by an order of magnitude, at 3.6 Ma (Rea, et al., 1998), which may have been associated with the uplift of the Tibetan Plateau and the cooling of the northern hemisphere. Continuous aeolian deposition in the present study region also began by this time, resulting in accumulation on the 'planation surface' (our basal age). After this time, this inner sub-basin of the Fenwei graben, which previously drained internally, became filled with fluvio-lacustrine sediments (the Sanmen Formation, illustrated in Fig. 4E) with a paleolake eventually covering much of the graben (Liu, 2004). This lake was then drained and the Sanmen gorge formed, initiating external drainage and linkage to the Yellow River system.

We suggest that the remarkable transition of the Fenwei graben, from filling to excavation (incision), was thus associated with the establishment of external drainage and the formation of the Sanmen gorge. The Xiaoshan barrier may have been breached by lake spillover as the ancestral fluvial system at its eastern front cut headward towards the Lingbao basin (Fig. 9C Ⅰ). Subsequently, following the emptying of the lake, fluvial incision into the sediments of the Sanmen Formation began (Fig. 9CⅡ). The geomorphic evidence indeed suggests that this drainage integration was associated with fluvial downcutting, from the 'planation surface' down to the level of the uppermost terrace (T5). The approximately synchronous development of this terrace both within the Sanmen gorge and further downstream at Kouma (see above), with dates of ~1.24 Ma and 1.2 Ma (respectively), indicates that the modern Yellow River had been established by this time and subsequently became entrenched (Fig. 9D). The formation of a river terrace staircase within the Fenwei graben is notable, implying that the graben interior is uplifting (a requirement for

terrace formation), albeit at a slower rate than the crust outside the faulted interior of the system (cf. Gao et al., 2016).

The initial development of the Sanmen gorge was thus an important event, since it marked the initiation of the eastward-flowing drainage of the Yellow River. Once this gorge had begun to form, terrigenous sediments could be transported from the interior of the Tibetan Plateau, in the upper reaches of the Yellow River, to the Bohai Gulf. Although loess began to accumulate in the present study region at significant rates by ~3.6 Ma, terrigenous sedimentation rates on the North China Plain and in the Bohai Gulf did not show dramatic increases until ~1.0 Ma (Xiao et al., 2008; Yao et al., 2010, 2012), in all probability in response to the formation of the Sanmen gorge. As Nie et al. (2015) have suggested, the majority of the sediment liberated by the dissection of the 'planation surface' from the middle and upper Yellow River basins was probably stored on the Chinese Loess Plateau before the through-going Yellow River drainage system was formed.

The formation of the Sanmen Gorge, which enabled through drainage from the upper Yellow River to the Bohai Gulf, would appear to have been the last in a series of linkage events joining inland basins. This progressive drainage linkage can now be envisaged to have occurred in sequence from upstream to downstream (contra Molnar, 2004), perhaps by means of repeated basin overflow in response to progressive basin filling coupled with increasing precipitation from the strengthening Asian Monsoon. The occurrence of this final eastern completion of the through-flowing Yellow River can also be demonstrated by the change in the type of zircon grains in the thick perched sedimentary sequence at Liujiahou (close to our site at Sanmenxia) reported by Kong et al. (2014), and called T5 by them. Zircon in the lower sediments here were of more local origin, whereas those from a sample high in the sequence (like those from later terrace sediments) were from upstream in the Yellow River, suggesting that basins upstream had been joined to form a through-flowing system by the time these uppermost sediments were deposited, just before incision by the newly-formed river and the development of the lower terrace staircase.

5.3. Wider comparisons

Similar sequences of events, whereby ancestral lake basins were disrupted and replaced by fluvial drainage, are also recognized in other continental interior regions

worldwide. For example, the history of integration of the upper reaches of the modern River Euphrates (in the eastern Anatolian Plateau) with the rest of its catchment, starting in the Mid-Pleistocene and associated with the disruption of paleolake basins, as investigated by Seyrek et al. (2008), Westaway et al. (2008), and Demir et al. (2009). Regional uplift of the eastern Anatolian Plateau and active faulting both played a part in this sequence of events. Another example, documented by Westaway et al. (2009), was the integration of the modern Rio Grande River in the central-southern USA. In that example the upper reaches of the ancestral river system drained into a paleolake in the Rio Grande Rift, an actively-developing graben; however, faster regional uplift following the Mid-Pleistocene Revolution resulted in disruption of this lake basin and the initiation of fluvial entrenchment, marked by dated river terraces, into its former interior. Numerous other examples of 'inverted' Late Cenozoic fluvio-lacustrine basins could be documented, including many reported by earlier FLAG research (e.g., Matoshko et al., 2004; Bridgland and Westaway, 2014) and in the present issue (Bridgland et al., 2016; Cunha et al., 2016; Maddy et al., 2016).

Attempts have recently been made to integrate onshore datasets indicating rates of erosion and offshore datasets indicating rates of deposition (e.g., Herman et al., 2013; Herman and Champagnac, 2016). It has been argued on the basis of increases in offshore sedimentation rates that accordingly terrestrial erosion rates increased (e.g., Zhang et al., 2001; Molnar, 2004). However, others have rejected the idea that erosion rates have increased in the Late Cenozoic (e.g., Willenbring and von Blanckenburg, 2010; Sadler and Jerolmack, 2015; Willenbring and Jerolmack, 2016). It has been shown here that the Yellow River and other major rivers only became integrated with their present catchment geometries in the relatively recent geological past, such that, beforehand, the products of erosion throughout much of these catchments were trapped in inland depocentres and were thus unable to reach the sea. This has to be considered as an important complicating factor in attempting comparison of global datasets of Late Cenozoic onshore erosion and offshore deposition.

6. Conclusions

Downcutting by the Yellow River into the Xiaoshan range, below a planation surface dated to ~3.63 Ma, has resulted in the formation of the Sanmen gorge. On the

basis of detailed field investigation, a new and uppermost Yellow River terrace, T5, has been recognized along the gorge. As a result, a sedimentary and geomorphic archive of five terraces was formed, in addition to the above-mentioned planation surface. Magnetostratigraphic records from the aeolian deposits accumulated on top of these surfaces provide a geochronological framework for this archive. The ages of the planation surface (P) and terraces T5, T4, T3, T2, and T1 have been determined at ~3.63 Ma, ~1.24 Ma, ~0.86 Ma, ~0.62 Ma, ~129 ka, and ~12 ka, respectively. Thus, the formation ages of the planation surface and uppermost terrace suggest that this gorge was entrenched primarily between 3.63 and 1.24 Ma. At the same time the landscape of the Fenwei region switched from basin filling to excavation ('basin inversion') enabling the formation of a series of terraces within the graben. Before the start of entrenchment of the Sanmen gorge, the products of erosion in the modern upper catchment of the Yellow River were 'trapped' inland and, therefore, unable to reach the sea. The dramatic increase in deposition rates in the Bohai Gulf, at the mouth of the modern Yellow River, at ~1.0 Ma, resulted from the integration of the Yellow River catchment following the initiation of drainage through Sanmen gorge and does not imply an increase in erosion rates at that time.

Acknowledgements

We are grateful to Xiaopeng Liu, Jian Zhang, and Prof. Qingyu Guan for assistance with the field sampling and laboratory analyses. The comments by Prof. Frank J. Pazzaglia, an anonymous referee, and the special issue editor, Stéphane Cordier, have led to considerable improvements and are gratefully acknowledged. This research is financially supported by the National Natural Science Foundation of China (Grant no. 41401001, 41571003), the Key Project of the Major Research Plan of the NSFC (Grant no. 91125008), the National Basic Research Program of China (2011CB403301), and the Fundamental Research Funds for the Central Universities.

References

AFSOM, 1988. Active fault system around Ordos Massif. Seismological Press, Beijing, pp. 77-136 (in Chinese).

An, Z., Kutzbach, J.E., Prell, W.L., Porter, S.C., 2001. Evolution of Asian monsoon and phased uplift of the Himalayan-Tibetan Plateau since Late Miocene times. Nature 411, 62-66.

Bridgland, D.R., 2000. River terrace systems in north-west Europe: an archive of environmental change, uplift and early human occupation. Quaternary Science Reviews 19, 1293-1303.

Bridgland, D.R., Westaway, R., 2008. Climatically controlled river terrace staircases: A worldwide Quaternary phenomenon. Geomorphology 98, 285-315.

Bridgland, D.R., Westaway, R., Abou Romieh, M., Candy, I., Daoud, M., Demir, T., Galiatsatos, N., Schreve, D., Seyrek, A., Shaw, A., White, T., Whittaker, J., 2012. The River Orontes in Syria and Turkey: Downstream variation of fluvial archives in different crustal blocks. Geomorphology 165-166, 25-49.

Bridgland, D.R., Westaway, R., 2014. Quaternary fluvial archives and landscape evolution: a global synthesis. Proceedings of the Geologists' Association 125, 600-629.

Bridgland, D.R., Demir, T., Seyrek, A., Abou Romieh, M., Daoud, M., Westaway, R., 2016. River terrace development in the NE Mediterranean region (Syria and Turkey): patterns in relation to crustal type. Quaternary Science Reviews.

Bull, W.B., 1990. Stream-terrace genesis: implication for soil development. Geomorphology 3, 351-367.

Cande, S.C., Kent, D.V., 1995. Revised calibration of the geomagnetic polarity timescale for the Late Cretaceous and Cenozoic. Journal of Geophysical Research 100,

6093-6095.

Cheng, S., Deng, Q., Zhou, S., Yang, G., 2002. Strath terraces of Jinshaan Canyon, Yellow River, and Quaternary tectonic movements of the Ordos Plateau, north China. Terra Nova 14, 215-224.

Clark, K.M., Schoenbohm, M.L., Royden, H.L., Whipple, X.K., Burchfiel, C.B., Zhang, X., Tang, W., Wang, E., Chen, L., 2004. Surface uplift, tectonics, and erosion of eastern Tibet from large-scale drainage patterns. Tectonics 23, TC1006, doi:10.1029/2002TC001402.

Clift, D.P., 2006. Controls on the erosion of Cenozoic Asia and the flux of clastic sediment to the ocean. Earth and Planetary Science Letters 241, 571-580.

Coltorti, M., Dramis, F., Ollier, D.C., 2007. Planation surfaces in Northern Ethiopia. Geomorphology 89, 287-296.

Craddock, H.W., Kirby, E., Harkins, W.N., Zhang, H., Shi, X., Liu, J., 2010. Rapid fluvial incision along the Yellow River during headward basin integration. Nature Geoscience 3, 209-213.

Cui, Z., Gao, Q., Liu, G., Pan, B., Chen, H., 1996. Planation surface, palaeokarst and uplift of Xizang (Tibet) Plateau. Science in China 39, 391-400.

Cunha, P.P., Martins, A.A., Buylaert, J.P., Murray, A.S., Raposo, L., Mozzi, P., Stokes, M., 2016. New data on the chronology of the Vale do Forno sedimentary sequence (Lower Tejo River terrace staircase) and its relevance as a fluvial archive of the Middle Pleistocene in western Iberia. Quaternary Science Reviews. http://dx.doi.org/10.1016/j.quascirev.2016.11.001.

Danišík, M., Kuhlemann, J., Dunkl, I., Székely, B., Frisch, W., 2006. Significance of high-elevated planation surfaces in interpreting thermotectonic evolution of the mountains. Goldschmidt Conference Abstracts A126.

Demir, T., Seyrek, A., Guillou, H., Scaillet, S., Westaway, R., Bridgland, D.R., 2009. Preservation by basalt of a staircase of latest Pliocene terraces of the River Murat in eastern Turkey: evidence for rapid uplift of the eastern Anatolian Plateau. Global and Planetary Change 68, 254-269.

Ding, Z., Liu, T. S., Liu, X. M., Chen, M. Y., An, Z. S., 1990. Thirty-seven climatic cycles in the last 2.5 Ma. Chinese Science Bulletin. 34, 1494-1496.

Ding, Z., Sun, J.M., Yang, S.L., Liu, T.S., 1998. Preliminary magnetostratigraphy of a thick eolian red clay-loess sequence at Lingtai, the Chinese Loess Plateau. Geophysical Research Letters. 25, 1225-1228.

Ding, Z., Derbyshire, E., Yang, S., Yu, Z., Xiong, S., Liu, T., 2002. Stacked 2.6-Ma grain size record from the Chinese loess based on five sections and correlation with the deep-sea $\delta^{18}O$ record. Paleoceanography 17, 1033-1053.

Dong, Y., Zhang, G., Neubauer, F., Liu, X., Genser, J., Hauzenberger, C., 2011. Tectonic evolution of the Qinling orogen, China: Review and synthesis. Journal of Asian Earth Sciences 41, 213-237.

Fan, D., Li, C., 2008. Timing of the Yangtze initiation during the Tibetan Plateau throughout to the East China Sea: A review. Front Earth Science China 2, 302-313.

Gao, H., Li, Z., Ji, Y., Pan, B., Liu, X., 2016. Climatic and tectonic controls on strath terraces along the upper Weihe River in central China. Quaternary Research 86, 326-334.

Geng X., 1981. Marine transgressions and regressions in East China since Late Pleistocene epoch. Acta Oceanologica Sinica 3, 114-130 (in Chinese, with English abstract).

Guo, Y., Zhang, J., Qiu, W., Hu, G., Zhuang, M., Zhou, L., 2012. Luminescence dating of the Yellow River terraces in the Hukou area, China. Quaternary Geochronology 10, 129-135.

He, P., Liu, L., Yu, Q., 1984. The age of the Sanmen series and the evolution of its depositional environment discussed in the light of the Dongpogou section in the Sanmen gorge area. Geological Reviews 30, 161-169 (in Chinese, with English abstract).

Herman, F., Champagnac, J.-D., 2016. Plio-Pleistocene increase of erosion rates in mountain belts in response to climate change. Terra Nova, 28, 2–10.

Herman, F., Seward, D., Valla, P.G., Carter, A., Kohn, B., Willett, S.D., Ehlers, T.A., 2013. Worldwide acceleration of mountain erosion under a cooling climate. Nature, 504, 423–426.

Huang, Z., Xu, M., Wang, L., Mi, N., Yu, D., Li, H., 2008. Shear wave splitting in the southern margin of the Ordos Block north China. Geophysical Research Letters 35, L19301. http://dx.doi.org/10.1029/2008GL035188.

Ji, J., Zheng, H., Li, S., Huang, X., 2006. The terraces of the Huanghe River in Pinglu County, Shanxi Province and their relationship with the disappearance of the Sanmen palaeolake and the formation of the Huanghe River. Quaternary Sciences 26, 665-672 (in Chinese, with English abstract).

Jiang, F., Fu, J., Wang, S., Sun, D., Zhao, Z., 2007. Formation of the Yellow River, inferred from loess-palaeosol sequence in Mangshan and lacustrine sediments in Sanmen Gorge, China. Quaternary International 175, 62-70.

Kirschvink, J.L., 1980. The least-squares line and plane and the analysis of palaeomagnetic data. Geophysical Journal International 62, 699-718.

Kong, P., Jia, J., Zheng, Y., 2014. Time constraints for the Yellow River traversing the Sanmen Gorge. Geochemistry, Geophysics, Geosystems 15, 395-407.

Kukla, G., An, Z.S., 1989. Loess stratigraphy in central China. Palaeogeography, Palaeoclimatology, Palaeoecology. 72, 203-225.

Kukla, G., Heller, F., Liu, M., Xu, C., Liu, S., An, S., 1988. Pleistocene climates in China dated by magnetic susceptibility. Geology 16, 811-814.

Li, J., 1991. The environmental effects of the uplift of the Qinghai-Xizang Plateau. Quaternary Science Reviews 10, 479-483.

Li, B., Sørensen, M.B., Atakan, K., 2015. Coulomb stress evolution in the Shanxi rift system, North China, since 1303 associated with coseismic, post-seismic and interseismic deformation. Geophysical Journal International 203, 1642-1664.

Lin, A.M., Yang, Z.Y., Sun, Z.M., Yang, T.S., 2001. How and when did the Yellow River develop its square bend? Geology 29, 951-954.

Liu, H., 2004. Formation and evolution of the Weihe River basin and uplift of the eastern Qinling Mountains, Ph.D. thesis, The Northeast University, Xian, China.

Liu, J., Zhang, P., Lease, R.O., Zheng, D., Wan, J., Wang, W., Zhang, H., 2013. Eocene onset and late Miocene acceleration of Cenozoic intracontinental extension in the North Qinling range-Weihe graben: Insights from apatite fission track thermochronology. Tectonophysics 584, 281-296.

Liu S., Li, G., Li, Y., Jin, J., 1988. The sedimentary characteristics of the North China plain as an indicator for the formation and evolution of the Yellow River. Henan Geology 6, 20-24 (in Chinese).

Liu, T., 1985. Loess and the Environment. China Ocean Press, Beijing, pp. 31-147.

Liu, X., Chen, B., 2000. Climatic warming in the Tibetan Plateau during the recent decades. International Journal of Climatology 20, 1729-1742.

Lu, H., Liu, X., Zhang, F., An, Z., Dodson, J., 1999. Astronomical calibration of loess-palaeosol deposits at Luochuan, central Chinese Loess Plateau.

Palaeogeography, Palaeoclimatology, Palaeoecology 154, 237-246.

Maddy, D., Veldkamp, A., Demir, T., van Gorp, W., Wijbrans, J.R., van Hinsbergen, D.J.J., Dekkers, M.J., Schreve, D., Schoorl, J.M., Scaife, R., Stemerdink, C., van der Schriek, T., Bridgland, D.R., Aytaç, A.S., 2016. The Gediz River fluvial archive: a benchmark for Quaternary research in Western Anatolia. Quaternary Science Reviews. http://dx.doi.org/10.1016/j.quascirev.2016.07.031.

Maher, B.A., Thompson, R., 1991. Mineral magnetic record of the Chinese loess and palaeosols. Geology 19, 3-6.

Matoshko, A., Gozhik, P., Danukalova, G., 2004. Key Late Cenozoic fluvial archives of eastern Europe: the Dniester, Dnieper, Don and Volga. Proceedings of the Geologists' Association 115, 141-173.

Miao, X., Lu, H., Li, Z., Cao, G., 2008. Paleocurrent and fabric analyses of the imbricated fluvial gravel deposits in Huangshui Valley, the northeastern Tibetan Plateau, China. Geomorphology. 99, 433-442.

Molnar, P., 2004. Late Cenozoic increase in accumulation rates of terrestrial sediment: how might climate change have affected erosion rates? Annu. Rev. Earth Planet. Sci. 32, 67–89.

Molnar, P., England, P., Martinod, J., 1993. Mantle dynamics, uplift of Tibetan Plateau, and the Indian Monsoon. Reviews of Geophysics 31, 357-396.

Nie, J., Stevens, T., Rittner, M., Stockli, D., Garzanti, E., Limonta, M., Bird, A., Ando, S., Vermeesch, P., Saylor, J., Lu, H., Breecker, D., Hu, X., Liu, S., Resentini, A., Vezzoli, G., Peng, W., Carter, A., Ji, S., Pan, B., 2015. Loess Plateau storage of Northeastern Tibetan Plateau-derived Yellow River sediment. Nature Communications 6, 1-8.

Ollier, C.D., Pain, C.F., 2000. The Origin of Mountains. Routledge, London.

Pan, B., Li, J., Chen, F., 1995. The Qinghai-Tibetan Plateau: Driver and amplifier of the global climate changes. I The characteristics of climate changes in Cenozoic. Journal of Lanzhou University (Natural Science Edition) 31, 120-128 (in Chinese, with English abstract).

Pan, B.T., Burbank, D., Wang, Y.X., Wu, G.J., Li, J.J., Guan, Q.Y., 2003. A 900 k.y. record of strath terrace formation during glacial-interglacial transitions in northwest China. Geology 32, 957-960.

Pan, B.T., Wang, J.P., Gao, H.S., Chen, Y.Y., Li, J.J., Liu, X.F., 2005a. Terrace dating as an archive of the run-through of the Sanmen Gorge. Progress in Natural Science. 15, 1096-1103.

Pan, B.T., Wang, J.P., Gao, H.S., Guan, Q.Y., Wang, Y., Su, H., Li, B.Y., Li, J.J., 2005b. Paleomagnetic dating of the topmost terrace in Kouma, Henan and its indication to the Yellow River's running through Sanmen Gorges. Chinese Science Bulletin. 50, 657-664.

Pan, B., Su, H., Hu, Z., Hu, X., Gao, H., Li, J., Kirby, E., 2009. Evaluating the role of climate and tectonics during non-steady incision of the Yellow River: evidence from a 1.24 Ma terrace record near Lanzhou, China. Quaternary Science Reviews 28, 3281-3290.

Pan, B.T., Hu, Z.B., Wang, J.P., Vandenberghe, J., Hu, X.F., 2011. A magnetostratigraphic record of landscape development in the eastern Ordos Plateau, China: Transition from Late Miocene and Early Pliocene stacked sedimentation to Late Pliocene and Quaternary uplift and incision by the Yellow River. Geomorphology 125, 225-238.

Pan, B.T., Hu, Z.B., Wang, J.P., Vandenberghe, J., Hu, X.F., Wen, Y.H., Li, Q., Cao, B., 2012. The approximate age of the planation surface and the incision of the Yellow River. Palaeogeography, Palaeoclimatology, Palaeoecology 356-357, 54-61.

Perrineau, A., van der Woerd, J., Gaudemer, Y., Jing, Z., Pik, R., Tapponnier, P.,

Thuizat, R., Zheng, R., 2011. Incision rate of the Yellow River in Northeastern Tibet constrained by ^{10}Be and ^{26}Al cosmogenic isotope dating of fluvial terraces: implications for catchment evolution and plateau building. In: Gloaguen, R., Ratschbacher, L. (Eds.), Growth and Collapse of the Tibetan Plateau. Special Publications of the Geological Society, London 353, 189-219.

Peulvast, J.P., Sales, V., 2004. Stepped surfaces and palaeolandforms in the northern Brazilian <Nordeste>: constraints on models of morphotectonic evolution. Geomorphology 62, 89-122.

Potter, P.E., 1978. Significance and origin of big rivers. Journal of Geology 86, 13–33.

Powell, C., Conaghan, P.J., 1973. Plate tectonics and the Himalayas. Earth and Planetary Science Letters 20, 1-12.

Prins, M.A., Zheng, H.B., Beets, K., Troelstra, S., Bacon, P., Kamerling, I., Wester, W., Konert, M., Huang, X.T., Wang, K.E., Vandenberghe, J., 2009. Dust supply from river floodplains: the case of the lower Huang He (Yellow River) recorded in loess-palaeosol sequence from the Mangshan Plateau. Journal of Quaternary Science 24, 75-84.

Rea, D., Snoeckx, H., Joseph, H.L., 1998. Late Cenozoic eolian deposition in the North Pacific: Asian drying, Tibetan uplift, and cooling of the northern hemisphere. Paleoceanography 13, 215-224.

Rixhon, G., Briant, R.M., Cordier, S., Duval, M., Jones, A., Scholz, D., 2016. Revealing the pace of river landscape evolution during the Quaternary: recent developments in numerical dating methods. Quaternary Science Reviews. http://dx.doi.org/10.1016/j.quascirev.2016.08.016

Rutter, N.W., Ding, Z.L., Evans, M.E., Liu, T.S., 1991. Baoji-type pedostratigraphic section, Loess Plateau, north-central China. Quaternary Science Review. 10, 1-22.

Sadler, P.M., Jerolmack, D.J., 2015. Scaling laws for aggradation, denudation and

898 progradation rates: the case for time-scale invariance at sediment sources and sinks.
899 Geological Society, London, Special Publications, 404, 69–88.
900
901 Saito, Y., Yang, Z., Hori, K., 2001. The Huanghe (Yellow River) and Changjiang
902 (Yangtze River) deltas: a review on their characteristics, evolution and sediment
903 discharge during the Holocene. Geomorphology 41, 219-231.
904
905 Schumm, S.A., Dumont, J.F., Holbrook, J.M., 2000. Active tectonics and alluvial river.
906 Cambridge University Press, Cambridge, UK, pp. 375-376.
907
908 Seyrek, A., Westaway, R., Pringle, M., Yurtmen, S., Demir, T., Rowbotham, G., 2008.
909 Timing of the Quaternary Elazığ volcanism, eastern Turkey, and its significance for
910 constraining landscape evolution and surface uplift. Turkish Journal of Earth Sciences
911 17, 497-541.
912
913 Soreghan, G.S., Elmore, R.D., Katz, B., Cogoini, M., Banerjee, S., 1997.
914 Pedogenically enhanced magnetic susceptibility variations preserved in Paleozoic
915 loessite. Geology 25, 1003-1006.
916
917 Stokes, M., 2008. Plio-Pleistocene drainage development in an inverted sedimentary
918 basin: Vera basin, Betic Cordillera, SE Spain. Geomorphology 100, 193-211.
919
920 Sun, Y., Clemens, C. S., An, Z., Yu, Z., 2006. Astronomical timescale and
921 palaeoclimatic implication of stacked 3.6-Myr monsoon records from the Chinese
922 Loess Plateau. Quaternary Science Reviews 25, 33-48.
923
924 Tapponnier, P., Xu, Z., Roger, F., Meyer, B., Arnaud, N., Wittlinger, G., Yang, J., 2001.
925 Oblique stepwise rise and growth of the Tibet Plateau. Science 294, 1671-1677.
926
927 Vandenberghe, J., Lu, H. Y., Sun, D. H., Huissteden, J., Konert, M., 2004. The late
928 Miocene and Pliocene climate in East Asia as recorded by grain size and magnetic
929 susceptibility of the Red Clay deposits (Chinese Loess Plateau). Palaeogeography,
930 Palaeoclimatology, Palaeoecology. 204, 239-255.
931

Vandenberghe, J., Wang, X., Lu, H., 2011. Differential impact of small-scaled tectonic movements on fluvial morphology and sedimentology (the Huang Shui catchment, NE Tibet Plateau). Geomorphology 134, 171-185.

Vandenberghe, J., de Moor, J.W. J., Spanjaard, G., 2012. Natural change and human impact in a present-day fluvial catchment: The Geul River, southern Netherlands. Geomorphology 159-160, 1-14.

Vandenberghe, J., 2016. From planation surfaces to river valleys. BSGLg 67, 93-106.

Veldkamp, A., van Dijke, J. J., 2000. Simulating internal and external controls on fluvial terrace stratigraphy: a qualitative comparison with the Mass record. Geomorphology 33, 225-236.

Wagner, T., Fritz, H., Stüwe, K., Nestroy, O., Rodnight, H., Hellstrom, J., Benischke, R., 2011. Correlations of cave levels, stream terraces and planation surfaces along the River Mur-Timing of landscape evolution along the eastern margin of the Alps. Geomorphology 134, 62-78.

Wang, S., Wu, X., Zhang, K., Jiang, F., Xue, B., Tong, G., Tian, G., 2001. Sedimentary records of environmental evolution in the Sanmen Lake Basin and the Yellow River running through the Sanmenxia Gorge eastward into the sea. Science in China 31, 585-608.

Wang, X., Lu, H., Vandenberghe, J., Zheng, S., van Balen, R., 2012. Late Miocene uplift of the NE Tibetan Plateau inferred from basin filling, planation and fluvial terraces in the Huang Shui catchment. Global and Planetary Change 88-89, 10-19.

Westaway, R., 2009. Active crustal deformation beyond the SE margin of the Tibetan Plateau: Constraints from the evolution of fluvial systems. Global and Planetary Change 68, 395-417.

Westaway, R., Demir, T., Seyrek, A., 2008. Geometry of the Turkey-Arabia and Africa-Arabia plate boundaries in the latest Miocene to Mid-Pliocene: the role of the

966 Malatya-Ovacık Fault Zone in eastern Turkey. eEarth, 3, 27-35.
967
968 Westaway, R., Bridgland, D.R., Sinha, R., Demir, T., 2009. Fluvial sequences as
969 evidence for landscape and climatic evolution in the Late Cenozoic: A synthesis of
970 data from IGCP 518. Global and Planetary Change 68, 237-253.
971
972 Willenbring, J.K., Jerolmack, D.J., 2016. The null hypothesis: globally steady rates of
973 erosion, weathering fluxes and shelf sediment accumulation during Late Cenozoic
974 mountain uplift and glaciation. Terra Nova 28, 11–18.
975
976 Willenbring, J.K., von Blanckenburg, F., 2010. Long-term stability of global erosion
977 rates and weathering during late-Cenozoic cooling. Nature 465, 211-214.
978
979 Wu, C., Xu, Q., Yang, X., 2000. Ancient drainage system of the Yellow River on
980 North China Plain. Journal of Geomechanics 6, 1-9 (in Chinese, with English
981 abstract).
982
983 Xia, D., Wu, S., Yu, Z., 1993. Changes of the Yellow River since the last glacial age.
984 Marine Geology & Quaternary Geology 13, 83-88 (in Chinese, with English abstract).
985
986 Xiao, G., Guo, Z., Chen, Y., Yao, Z., Shao, Y., Wang, X., Hao, Q., Lu, Y., 2008.
987 Magnetostratigraphy of BZ_1 borehole in west coast of Bohai bay, northern China.
988 Quaternary Sciences 28, 909-916 (in Chinese, with English abstract).
989
990 Xue, D., 1996. A humble option of the formed age for the eastern section of the
991 Yellow River. Henan Geology 14, 110-112 (in Chinese, with English abstract).
992
993 Yang, H., Chen, X., 1985. Quaternary transgressions, eustatic changes and shifting of
994 shoreling in East China. Marine Geology & Quaternary Geology 5, 59-80 (in Chinese,
995 with English abstract).
996
997 Yang, S., Cai, J., Li, C., Deng, B., 2001. New discussion about the run-through time
998 of the Yellow River. Marine Geology & Quaternary Geolgoy 21, 15-20 (in Chinese,
999 with English abstract).

Yao, Z., Xiao, G., Wu, H., Liu, W., Chen, Y., 2010. Plio-Pleistocene vegetation changes in the North China Plain: Magnetostratigraphy, oxygen and carbon isotopic composition of pedogenic carbonates. Palaeogeography, Palaeoclimatology, Palaeoecology 297, 502-510.

Yao, Z., Guo, Z., Xiao, G., Wang, Q., Shi, X., Wang, X., 2012. Sedimentary history of the western Bohai coastal plain since the late Pliocene: Implications on tectonic, climatic and sea-level changes. Journal of Asian Earth Sciences 54-55, 192-202.

Yu, H., 1999. Ages of the Yellow River delta in shelf regions of the Yellow sea and the Bohai sea. Journal of Geomechanics 5, 80-88 (in Chinese, with English abstract).

Yuan, Y., Hu, S., Wang, H., Sun, F., 2007. Meso-Cenozoic tectonothermal evolution of Ordos Basin, central China: Insight from newly acquired vitrinite reflectance data and a revision of existing paleothermal indicator data. Journal of Geodynamics 44, 33-46.

Yue, L., Zhang, Y., Wang, J., Deng, X., Zhang, L., 1999. Magnetostratigraphic sequence of continental deposits in Northern China since 5.3 Ma. Geological Reviews 45, 444-448 (in Chinese, with English abstract).

Zhang, J., Qiu, W., Wang, X., Hu, G., Li, R., Zhou, L., 2010. Optical dating of a hyperconcentrated flow deposit on a Yellow River terrace in Hukou, Shaanxi, China. Quaternary Geochronology 5, 194-199.

Zhang, P., Molnar, P., Downs, W.R., 2001. Increased sedimentation rates and grain sizes 2-4 Myr ago due to the influence of climate change on erosion rates. Nature 410, 891–897.

Zhang, Y., Mercier, J.L., Vergély, P., 1998. Extension in the graben systems around the Ordos (China), and its contribution to the extrusion tectonics of south China with respect to Gobi-Mongolia. Tectonophysics 285, 41-75.

Zhang, Y., Ma, Y., Yang, N., Shi, W., Dong, S., 2003. Cenozoic extensional stress evolution in North China. Journal of Geodynamics 36, 591-613.

Zheng, H., Powell, C., Rea, D., Wang, J., Wang, P., 2004. Late Miocene and mid-Pliocene enhancement of the East Asian monsoon as viewed from land and sea. Global and Planetary Change 41, 147-155.

Zheng, H., Huang, X., Ji, J., Liu, R., Zeng, Q., Jiang, F., 2007. Ultra-high rates of loess sedimentation at Zhengzhou since Stage 7: Implication for the Yellow River erosion of the Sanmen Gorge. Geomorphology 85, 131-142.

Zheng, H., Clift, P., Wang, P., Tada, R., Jia, J., He, M., Jourdan, F., 2013. Pre-Miocene birth of the Yangtze River. PNAS 110, 7556-7561.

Zhu, H., Chen, K., Liu, K., He, S., 2008. A sequence stratigraphic model for reservoir sand-body distribution in the Lower Permian Shanxi Formation in the Ordos Basin, Northern China. Marine and Petroleum Geology 25, 731-743.

Zhu, R. X., Laj, C., Mazaud, A., 1994. The Matuyama-Brunhes and upper Jaramillo transitions recorded in a loess section at Weinan, north-central China. Earth and Planetary Science Letters. 125, 143-158.

Table Captions

Table 1. Fluvial terrace correlation between Sanmenxia and Kouma

Figure Captions

Fig. 1. Map of the Fenwei graben and its surroundings, showing faults (from AFSOM, 1998), rivers, topography, and the locations of the four sub-basins (the Weihe, Lingbao, Yuncheng, and Fenhe basins). The locations of Figs 2 and 3 are also indicated. The inset map shows the major fault systems, plate motions, Bohai Gulf, and location within China.

Fig. 2. Maximum, mean, and minimum topography along a 50-km-wide swath along the Sanmen gorge (see Fig. 1 for location). Active faults and the interpreted long profile of the planation surface are also depicted (see also Fig. 4).

Fig. 3. Map of the study region showing topography (using the same data source as Fig. 1), active faults, and field locatities (see Fig. 1 for location).

Fig. 4. Field photos of the Sanmen gorge and its entrance. (A) View of the planation surface dominating the Xiaoshan along the Sanmen gorge, looking east from 34°51′09.36″ N, 111°19′34.16″E. (B) The westward dip of the planation surface (looking north from 34°46′03.27″ N, 111°17′53.48″E), the result of deformation close to the inlet of the Sanmen gorge. (C and D) Fluvial terrace staircase at Sanmenxia, looking west (C) and south (D). Five terraces have been identified below the planation surface, of which the uppermost (T5) is newly recognized. (E) Closeup view of the sedimentary sequence forming terrace T2 at Sanmenxia (see (D) for location). The fluvio-lacustrine Sanmen Formation, characterized by horizontally bedded mudstone, siltstone, clay, conglomerate, and sandstone, crops out below the terrace gravel.

Fig. 5. Transverse profiles through the fluvial terrace staircases at the field localities (Zhangbian, Sanmenxia, Dongcun, Xiaolangdi, and Kouma; see Fig. 3 for locations). Note that the terrace staircases at Zhangbian, Sanmenxia and Dongcun are affected by normal faulting.

Fig. 6. Interpreted longitudinal profile of terrace levels along the Sanmen gorge, using height data from Table 1. The normal faults that define the ends of the gorge are depicted in Fig. 2 and 3.

Fig. 7. Magnetostratigraphy and pedostratigraphy of the aeolian deposits overlying the fluvial terraces and planation surface at Sanmenxia. These TL dates for T2 and interpreted chrons (black for normal geomagnetic polarity, white for reverse) for terraces T4, T3, and T2 are all from Pan et al. (2005a). For the newly recognized terrace T5 and the planation surface, paleomagnetic data from the overlying ~130-m- and 152-m-thick aeolian deposits are used to obtain age interpretations (of ~1.24 Ma and 3.63 Ma, respectively), using the Cande and Kent (1995) geomagnetic polarity timescale. However, these data are displayed here without filtering for noise. The magnetic susceptibility values are higher in the palaeosol units than those in the neighboring loess layers.

Fig. 8. A selection of the data from Fig. 7, illustrating the thermal demagnetization process used to identify the primary components of rock magnetization that indicate the polarity of the Earth's magnetic field at the time of deposition. For each figure part, the left-hand panel shows the horizontal (solid symbols) and vertical (open symbols) components of rock magnetization, whereas the right-hand panel shows how the strength of magnetization decreases with increasing temperature. (A) Sample PR-10.0 from the 10.0-m thickness of the aeolian section on the planation surface, a sample of Carbonate nodules. After a low-temperature overprint is removed, this sample is seen to be magnetized upward and southward, indicating reverse polarity. (B) Sample PR-0.5 from 0.5-m thickness of the aeolian section on the planation surface, a sample of Red Clay. After a low-temperature overprint is removed, this sample is seen to be magnetized downward and northward, indicating normal polarity. (C) Sample PL-69.0 from 69.0-m thickness of the aeolian section on the planation surface, a sample of loess. After a substantial overprint is removed, this sample is seen to be magnetized upward and southward, indicating reverse polarity. (D) Sample PL-109.0 from 109.0-m thickness of the aeolian section on the planation surface, a sample of loess. This sample is seen to be magnetized downward and northward, indicating normal polarity. (E) Sample T5-33.0 from 33.0-m thickness of the loess section on terrace T5.

This sample is seen to be magnetized downward and westward, indicating ambiguous polarity. (F) Sample T5-28.0 from 28.0-m thickness of the loess section on terrace T5. This sample is seen to be magnetized downward and northward, indicating normal polarity.

Fig. 9. Schematic diagram illustrating landscape evolution within the Fenwei graben. (A) The initial downfaulting, erosion, and filling of the Fenwei graben. (I) Development, in the Early Pliocene, of the graben as a result of extensional tectonism. (II) Planation, circa 3.6 Ma (according to the magnetostratigraphic data), during infilling of the graben, marked by emplacement of the lower part of the Sanmen Formation. (B) Uplift and dissection of the planation surface after ~3.6 Ma. At this time the extension switched from the initial set of normal faults to a newer set in the hanging-walls of the initial set, resulting in narrowing of the graben. (C) Erosion, fill, and excavation of this narrower graben. (I) Erosion and fill when the narrower graben was occupied by an isolated fluvio-lacustrine system, during deposition of the upper part of the Sanmen Formation in the Early Pleistocene. (II) Initial entrenchment of the Yellow River into the Sanmen Formation circa 1.2 Ma. At this time the former lake basin was disrupted and fluvial drainage first developed from west to east across the Xiaoshan, leading to the formation of the Sanmen gorge and incision into the Sanmen Formation. (D) Incision and terrace formation by the Yellow River at Sanmenxia since the late Early Pleistocene, creating the present fluvial terrace staircase.

The linking of the upper-middle and lower reaches of the Yellow River as a result of fluvial entrenchment

ZhenBo Hu[a,] *, BaoTian Pan[a,] *, David Bridgland[b], Jef Vandenberghe[c], LianYong Guo[a], YunLong Fan[a], Rob Westaway[d]

[a]Key Laboratory of Western China's Environmental Systems (Ministry of Education), College of Earth and Environmental Sciences, Lanzhou University, Lanzhou 730000, People's Republic of China

[b]Department of Geography, Durham University, South Road, Durham DH1 3LE, UK

[c]Department of Earth Sciences, Vrije Universiteit, De Boelelaan 1085, 1081 HV Amsterdam, The Netherlands

[d]School of Engineering, University of Glasgow, James Watt (South) Building, Glasgow G12 8QQ, UK

*Corresponding author. E-mail: zhbhu@lzu.edu.cn; hu_zhb@126.com (Z. Hu)

Abstract

The upper–middle Yellow River flows through the Fenwei graben, a structure resulting from extensional tectonism that was formed and repeatedly extended during the Cenozoic. The drainage system within this graben was formerly isolated from the lower reaches of the Yellow River system by the Xiaoshan mountains, an actively growing ~NW–SE trending range. The modern course of the Yellow River takes it through this range along the Sanmen gorge, the formation of which was of great significance in that it initiated through-going drainage between the upper–middle and lower reaches of the system. The timing of this event, which was clearly a criticial point in the evolution of the Yellow River, can be established by dating the terraces in the gorge. Intermittent deepening of this gorge by the Yellow River from a high-level planation surface capping the mountain range has resulted in the formation of five terraces. Magnetostratigraphic records from aeolian deposits accumulated on these surfaces provide a geochronological sequence for this geomorphic archive, in which the ages of the planation surface and of terraces T5, T4, T3, T2, and T1 have been determined as ~3.63 Ma, ~1.24 Ma, ~0.86 Ma, ~0.62 Ma, ~129 ka, and ~12 ka, respectively.

Under the constraint of this chronological framework, a model for landscape evolution is proposed here. Uplift of the inner Fenwei graben and of the surrounding mountain ranges led to dissection of the 3.63 Ma old planation surface in conjunction with the formation of the Sanmen gorge. Drainage of the lake previously occupying the basin would have promoted incision into the fluvio-lacustrine graben sediments; indeed, gorge formation through the Xiaoshan may have been initiated or intensified by lake overflow. The ages obtained for the planation surface and uppermost terrace suggest that the formation of the Sanmen gorge and the initiation of the through-going eastward drainage of the Yellow River occurred between 3.63 and 1.24 Ma. Before the start of gorge entrenchment, the products of erosion in the modern upper catchment of the Yellow River were unable to reach the sea. The dramatic increase in deposition rates in the Bohai Gulf (at the mouth of the modern Yellow River in the East China Sea), ~1.0 Ma ago, thus resulted from the initiation of an integral (enlarged) Yellow River catchment drainage through the Sanmen gorge; it does not imply an increase in erosion rates at that time.

*Keywords***:** Yellow River; Sanmen gorge; Fenwei graben; Terrace; Planation surface; Fluvial incision rate

1. Introduction

Many of the world's largest rivers flow along structural lows and major rift systems (Potter, 1978) and, meanwhile, have shaped the landscape over large areas. In those regions that have been entrenched, the interaction between climate, uplift, lithology, and base level have been fundamental controls on the evolution of fluvial systems (Schumm et al., 2000; Veldkamp and van Dijke, 2000; Pan et al., 2003; Bridgland and Westaway, 2008; Vandenberghe et al., 2011). Moreover, information about tectonic activity and climatic change can be imprinted into sedimentary and morphological fluvial archives (e.g., Bridgland, 2000; Stokes, 2008; Westaway, 2009; Craddock et al., 2010; Bridgland et al., 2012; Bridgland and Westaway, 2014). The development of large rivers is thus widely employed to determine the history of structural, environmental, and topographical change during the Quaternary. ~~(An et al., 2001; Westaway et al., 2009; Bridgland and Westaway, 2014; Hu et al., 2016). The specific objective of this paper is to reconstruct the eastward drainage history of the Yellow River by dating its terraces in the critical reach between its middle and lower catchments (the Sanmen gorge).~~

The formation of the Tibetan Plateau is generally thought to have been an amplifier and driver for the environmental evolution of East Asia, strengthening the East Asian monsoon and thus having an influence on precipitation and related erosion rates (Li, 1991; Pan et al., 1995; Liu and Chen, 2000). Constraint on its uplift history provides the basis for understanding the effects of high topography on climate and on various earth surface processes (An et al., 2001).

T~~1.1. The significance of fluvial archives in reconstructing East Asian landscape evolution~~

~~T~~he development of fluvial systems in East Asia has also been closely associated with topographical evolution since the India–Eurasia collision (e.g., Powell and Conaghan, 1973; Lin et al., 2001; Fan and Li, 2008). The eastward flow direction of the largest rivers in China (e.g., the Yellow River and the Yangtze) is generally attributed to the relative eastward decline of the macro-relief, resulting from the uplift of the Tibetan Plateau (Miao et al., 2008; Craddock et al., 2010; Zheng et al., 2013). Marine accumulation of terrigenous sediments derived from these large fluvial systems may be assumed to have started in the Bohai Gulf immediately after the

Formatted: Indent: First line: 2 ch

Formatted: Indent: First line: 0 ch

formation of this drainage pattern (Zheng et al., 2004; Jiang et al., 2007). ~~These continuous terrigenous sediment stacks within marine basins are generally believed to provide an important record of climatically- and tectonically-controlled mountain denudation history and to play a key role in the understanding of Quaternary surface uplift and global cooling (Clift, 2006; Willenbring and von Blanckenburg, 2010).~~ The establishment of these eastward-flowing drainage systems ~~thus~~ provides a critical link between upland erosion and the marine accumulation of terrigenous sediments (Nie et al., 2015). Despite much attention having been paid to long-term fluvial landscape development in East Asia, which is related to the uplift of the Tibetan Plateau during the Quaternary ~~(see below)~~, the formation age of the eastward drainage pattern in China is still strongly debated (cf. Lin et al., 2001; Clark et al., 2004; Pan et al., 2005b; Clift, 2006; Zheng et al., 2007, 2013). It is the specific objective of this paper to reconstruct the eastward drainage history of the Yellow River by dating its terraces in the critical reach between its middle and lower catchments. The formation ages of terraces T4, T3 and T2 at Sanmenxia were determined previously by Pan et al. (2005a) as 0.86 Ma, 0.62 Ma, and 0.129 Ma, respectively, but no dating was available for the highest terrace T5 and the planation level in the study region.

~~1.~~2. Regional geological and geomorphic setting

Formatted: Font: Bold

2.1. General position of the Ordos block, Fenwei graben and Xiaoshan mountains

Formatted: Indent: First line: 0 ch

~~The motion, during the Cenozoic, of the Indian plate relative to Eurasia led to crustal shortening and the formation of the Tibetan Plateau (Molnar et al., 1993; Royden et al., 2008; White and Lister, 2012). This major positive topographical feature is generally thought to have been an amplifier and driver for the environmental evolution of East Asia, strengthening the East Asian monsoon and thus having an influence on precipitation and related erosion rates (Li, 1991; Pan et al., 1995; Liu and Chen, 2000; Molnar et al., 2010). Constraint on its uplift history provides the basis for understanding the effects of high topography on climate and on various Earth surface processes (Ruddiman and Kutzbach, 1989; An et al., 2001; G. Pan et al., 2012). Owing to an insufficiently reliable chronological framework, however, the relationship between paleoenvironmental conditions and landscape evolution is still poorly~~

~~understood (Molnar et al., 2010).~~

The Ordos block is an upland massif located at the northeastern margin of the Tibetan Plateau~~,~~ and bounded by graben systems. During the Mesozoic, this block was a large basin with an area of ~320,000 km^2 (Zhu et al., 2008) and was filled with terrigenous clastic sediments. Following the Indo-Asian collision (Molnar et al., 1993), deformation progressively propagated from the collision zone to the northeastern margin of the Tibetan Plateau (Tapponnier et al., 2001; Fig. 1, inset). Arc-shaped thrust faults and strike-slip fault systems were thus generated between the Ordos block and the Tibetan Plateau, leading to the formation, by extensional stress, of the crescent~~S~~-shaped Fenwei graben (Zhang et al., 1998, 2003; Huang et al., 2008; Liu et al., 2013). Meanwhile, the Ordos block and the Qinling, Huashan, Luliang, and Taihang (including the Xiaoshan) mountains were uplifted with respect to this subsiding graben (AFSOM, 1988). In the middle reaches of the Yellow River, the landscape is characterized by a topography of alternating depressions and rolling uplands, consisting of the above-mentioned ranges. Apatite fission track data and geomorphic chronology have indicated that this area was uplifted in the early Miocene and was then planated by the late Neogene (Yuan et al., 2007; Pan et al., 2012).

<Fig. 1 hereabout>

The Fenwei graben is a NE–SW trending, crescent-shaped subsided area constrained by numerous normal and strike-slip faults, covering more than 20,000 km^2 (AFSOM, 1988; Fig. 1). Its basement is further intersected by internal ENE-trending normal faults, forming four sub-basins, the Weihe, Fenhe, Yuncheng, and Lingbao basins (Fig. 1). The Fenwei graben is generally considered to have been an extensional area that was continuously subsiding during the Cenozoic, a response to the eastward extrusion of the Tibetan Plateau (Zhang et al., 1998, 2003); it has simultaneously been filled by ~4000 m of fluvio-lacustrine deposits (AFSOM, 1988). Based on previous investigation, these sediments dominate most of the graben, implying the existence of a large lake, from Sanmenxia in the east, Baoji in the west, the Qinling mountains in the south, and Yumenkou in the north (Liu, 2004; Fig. 1). These fluvio-lacustrine sediments are defined as the Sanmen Formation, characterized by undeformed, generally horizonal and parallel lithostratigraphy (AFSOM, 1988),

pointing to regular vertical subsidence.

<Fig. 2 hereabout>

Subsidence, extensional tectonics and uplift have remained vigorous and active during the Quaternary in the area of the Fenwei graben. Fault scarps and triangular facets that can be traced for hundreds of kilometers are readily observed along the northern front of the Qinling, Huashan, and the southern front (Xiaoshan) of the Taihang Mountains (Dong et al., 2011). Major earthquakes around this graben are known from historical records (Zhang et al., 2003). The middle and lower reaches of the Yellow River are separated by the Xiaoshan mountains. To cross this topographic barrier the Yellow River has incised deeply into these mountains, creating the Sanmen gorge, between Sanmenxia and Xiaolangdi (Fig. 2 and Fig. 3). The Sanmen gorge~~, through which the Yellow River traverses the Xiaoshan Mountain Range (thus linking the graben with river system further downstream),~~ is constrained by normal and strike-slip faults (Fig. 2), and is transected by numerous inferred inner faults (Fig. 3). Many ground fissures associated with earthquakes are exposed along these inferred faults within the gorge, indicating that uplift of the Xiaoshan with respect to the Lingbao basin, to the northwest, and the North China Plain (to the southeast) has never ceased (AFSOM, 1988).

<Fig. 3 hereabout>

The modern landscape in the vicinity of the Sanmen gorge is an uplifted and rolling surface that is well preserved on resistant rocks in the higher parts of the area. It represents a remnant of a planation surface that was cut through most of the pre-existing tectonic structures and the relief right across the Lingbao basin, the Xiaoshan range, and the North China Plain (Fig. 4A). This geomorphic surface was deformed strongly over the Xiaoshan (Fig. 4B), forming a convexity between the Lingbao basin and the North China Plain (Fig. 2). In general, its altitude exhibits a declining trend towards the east, falling below~~reaching less than~~ 400 m in the North China Plain.

<Fig. 4 hereabout>

21.23. The downstream part of the Yellow River~~Yellow River catchment and its relation with the Sanmen gorge~~

~~Here we focus upon T~~the Yellow River (Huanghe)~~, one of the largest in the world, which~~ originating~~s~~ from the northeastern margin of the Tibetan Plateau and flowing~~s~~ eastwards across China, crossesing numerous tectonic zones and major active faults. ~~and finally debouching, with its huge sediment load, into the Bohai Gulf (Saito et al., 2001).~~ The Xiaoshan mountain range represents the final barrier to be crossed by the river before it flows across the North China Plain and finally debouches, attaining a total length of 5464 km (Wang et al., 2001), with its huge sediment load, into the Bohai Gulf (Saito et al., 2001; ~~This large fluvial system represents an exceptional opportunity in that the relationship between terrigenous records within offshore marine basins and inland landscape evolution can be potentially evaluated with reference to Yellow River fluvial archives, which provide an excellent age constraint on the evolution of the eastward flowing drainage pattern.~~

~~In the transition zone between middle and lower reaches of the Yellow River, rapid fluvial incision has been initiated into the Xiaoshan mountains, an actively growing ~NW–SE trending range, to form the aforementioned Sanmen gorge, an incised valley between Sanmenxia and Xiaolangdi (Fig. 2 and Fig. 3). The Xiaoshan mountain range represents effectively the final barrier to be crossed by the Yellow River in its eastward flow to the Bohai Gulf (~~Fig. 1, inset). ~~; downstream of the Sanmen gorge, the river flows to the coast across the North China Plain (Fig. 1), attaining a total length of 5464 km (Wang et al., 2001).~~ The North China ~~is~~ P~~p~~lain, which was formed from the steady supply of sediments from the upper and middle reaches of the Yellow River~~. It~~ has remained close to sea level throughout the Quaternary (Yang and Chen, 1985), experiencing marine inundation during some interglacial periods (Geng, 1981). Sedimentary cores from this plain were analyzed in an attempt to identify the oldest fluvial sediments from the Yellow River, thereby dating the initiation of its eastward flow (Liu et al., 1988). However, the river has a long history of wandering in disparate courses across the North China Plain, resulting in deposition at different times at different sites, which has led to estimates for the date of eastward-drainage initiation that range from Early to Late Pleistocene (Xia et al., 1993; Yu, 1999; Wu et al., 2000; Yang et al., 2001).

226

227 21.34. The evolution of the Yellow River and its relation with the Fenwei graben and
228 the Sanmen gorge
229
230 It has been shown previously that the area upstream of the Sanmen gorge, which
231 coincides with The extensional Fenwei graben, situated upstream of the Sanmen
232 gorge, structure, was occupied, before the formation of the Yellow River, by a lake that
233 covered the Weihe, Fenhe, Yuncheng, and Lingbao basins (Liu, 2004). According to
234 the distribution of fluvio-lacustrine sediments, the eastward flow of the Yellow River
235 through and downstream from this palaeolake suggests that the river was instrumental
236 in the overflow, drainage and consequent disappearance of the lake (Wang et al., 2001;
237 Zhang et al., 2016). The ages of the uppermost fluvio-lacustrine sediments within
238 these basins range from 1.85 Ma to 150 ka (He et al., 1984; Yue et al., 1999; Ji et al.,
239 2006), representing an somewhat imprecise chronological framework for the
240 formation of the eastward drainage pattern of the Yellow River through the Sanmen
241 gorge. Furthermore, recent work using cosmogenic nuclide dating, combined with
242 provenance analysis of zircon and U–Pb age distributions, suggests that the Sanmen
243 gorge was initially entrenched, during the period from 1.5 to 1.3 Ma, by the eastward
244 draining Weihe River, which is now the largest tributary of the Yellow River (Kong et
245 al., 2014). Comparative analysis of ostracod assemblages (Lishania) from the
246 fluvio-lacustrine sediments in the Fenwei graben and from the fluvial sediments in the
247 North China Plain suggests a close correlation between the two areas after ~1.0 Ma,
248 implying the existence of eastward drainage by that time (Xue, 1996). Finally, loess
249 stratigraphy at Mangshan, ~100 km downstream of the Sanmen gorge (Fig. 2), shows
250 a dramatic increase in the loess accumulation rate of loess since the formation of
251 palaeosol S2 (Prins et al., 2009). wasThis increase is suggested to result from a
252 proximal contribution of silt blown from the Yellow River floodplain, further
253 suggesting that eastward drainage had been formed at the latest by least c.by 243 ka,
254 which is the formation age of S2 (Jiang et al., 2007; Zheng et al., 2007; Prins et al.,
255 2009), the age of palaeosol S2.
256
257 1.5. Dating the formation of the Sanmen gorge
258
259 An important objective of this paper is to reconstruct the eastward drainage

Formatted: English (United States)
Formatted: English (United States)
Formatted: English (United States)
Formatted: Indent: First line: 0 ch

history of the Yellow River within a geochronological framework.~~In general, the~~ The initiation of th~~e~~is eastward draining r~~Yellow R~~iver has remained a highly controversial topic. Given that river terraces, as former floodplains (Bull, 1990; Merritt et al., 1994), can provide compelling evidence for determining drainage development (Stokes, 2008; Westaway et al., 2009; Vandenberghe et al., 2011), the dating of such terraces along the Sanmen gorge can provide important evidence (Pan et al., 2005a; Zheng et al., 2007; Kong et al., 2014). M~~Here, m~~ost of the terraces in the gorge are directly overlain by thick aeolian loess covers, which can offer an excellent age control for the underlying terraces sediments (e.g., Liu, 1985; Pan et al., 2009, 2012; Guo et al., 2012). The chronological framework from these loess covers has been based on a combined approach of magnetostratigraphy, pedostratigraphy, electron spin resonance (ESR), and luminescence dating, and cosmogenic radionuclide geochronology (e.g., Cheng et al., 2002; Pan et al., 2009; Craddock et al., 2010; Zhang et al., 2010; Perrineau et al., 2011). From the constraint provided by the loess stratigraphy, the age of the highest Yellow River terrace at the downstream end of the Sanmen gorge was determined at 1.2 Ma by Pan et al. (2005b). In contrast, the oldest terrace at the gorge inlet was considered significantly younger, at only 0.8 Ma (Pan et al., 2005a). This temporal mismatch may be attributed to incomplete age control from the loess covers in the gorge.

~~The specific objective of this paper is to reconstruct the eastward drainage history of the Yellow River within a geochronological framework.~~ A series of well-preserved terraces was formed by the Yellow River in the Sanmen gorge during its incision into the Xiaoshan. Here, detailed field investigation was performed to establish a complete sequence of geomorphic surfaces. Next, a new geochronology for the geomorphic archive is presented, based on the combined approach of magnetostratigraphy, pedostratigraphy, and optically stimulated luminescence (OSL) dating of the aeolian cover on the geomorphic surfaces. Finally, this geochronology is used to constrain the formation age of the eastward-draining Yellow River.

<Fig. 5 hereabout>

3~~2~~. Method

3~~2~~.1. Field research

Intermittent downcutting by the Yellow River, starting from the planation surface and cutting into the bedrock of the Xiaoshan to form the Sanmen gorge, has given rise to a series of terraces along the valley. Field observations suggest that these terrace treads are generally disposed asymmetrically within the valley. To elucidate the formation history of the Yellow River within this gorge, work has focused on five geomorphic cross-sections, from Zhangbian to Kouma (Fig. 3). For each cross-section, terraces below the planation surface were identified and their tread heights (top of fluvial deposits) above river level determined, the characteristics of the fluvial deposits were described, and the thickness of overlying aeolian sediments (loess and Red Clay) was measured.

<Table 1 hereabout>

The five transect sites were selected as representative of the supposed relict planation surface and of the suite of lower-level fluvial terraces. The transect at Zhangbian is located within the Lingbao basin. The~~se~~ transects at Sanmenxia, Dongcun, and Xiaolangdi are located, respectively, at the inlet of, within, and at the outlet of the gorge, whereas the Kouma site is ~20 km downstream of the gorge (Fig. 3). Field measurements of terrace elevation and the thickness of overlying aeolian cover were performed using a differential GPS system with an uncertainty of < 5 cm. According to these results, combined with loess stratigraphy and geomorphic surface tracking, terrace sequences at these sites were outlined (Fig. 5) and correlated (Table 1). It appears that the altitude of the planation surface and the vertical separation~~s~~ between high terrace treads and the present-day river level increase~~s~~ considerably at first and then gradually decrease~~s~~ with downstream distance along the gorge (Fig. 6). This topographical pattern corresponds with the convexity, mentioned above, thought to relate to the active uplift of the Xiaoshan range.

<Fig. 6 hereabout>

3~~2~~.2. Aeolian deposits capping the geomorphic surfaces

The aeolian sediments (Tertiary Red Clay and overlying Quaternary loess)

covering the planation surface and terrace treads provide valuable age estimates for the underlying landforms. However, the aeolian covers are rather thin at Dongcun and Xiaolangdi in comparison with those at Zhangbian, Sanmenxia, and Kouma, probably because accumulation was less in the confined Sanmen gorge (Fig. 5). Thus the Sanmenxia transect was selected for the analysis of magnetostratigraphy and~~,~~ pedostratigraphy~~, and OSL geochronology~~ of the aeolian sequence.

With reference to the established timescale of the aeolian sedimentary sequence on the Chinese Loess Plateau, enhanced by astronomical tuning and paleomagnetism, the basal ages of aeolian cover on each terrace along the Sanmen gorge can be determined. Readers are~~can be~~ referred to Ding et al. (2002) for a detailed chronostratigraphic framework of the Chinese loess. Thus~~erefore,~~ these aeolian series, in combination with their magnetostratigraphic and pedostratigraphic properties, provide a geochronological framework for the terrace sequences in the five Yellow River transects, as will now be described. The present study concentrates on the, hitherto undated, aeolian deposits above the planation surface and terrace T5.~~Since the formation ages of terraces T4, T3 and T2 at Sanmenxia were determined previously by Pan et al. (2005a) as 0.86 Ma, 0.62 Ma, and 129 ka, respectively, the present study concentrates on samples of aeolian deposits above the planation surface, terrace (T5), and the lowermost (T1) terrace.~~

3~~2~~.3. Magnetic susceptibility measurements

Magnetic susceptibility reflects the layering of loess and palaeosols (Soreghan et al., 1997) and thus can further confirm the identification of pedostratigraphic units and aid correlation. Powder samples were taken at 0.05-m intervals from the aeolian covers of the planation surface and uppermost terrace (T5). A total of 5650 samples were air-dried in the laboratory and then gently ground. Measurements with a Bartington MS2B magnetic susceptibility meter were used to obtain the mass magnetic susceptibility (Fig. 7).

<Fig. 7 hereabout>

3~~2~~.4. Paleomagnetism

Samples were taken from the 152-m and 130.5-m thick aeolian deposits accumulated respectively on top of the planation surface and the uppermost terrace (T5). A total of 441 oriented block samples were collected at 0.25-m intervals in the Red Clay and at intervals of ~0.5–3.0 m in the loess. In the laboratory these samples were cut into 2-cm^3 transects, producing three sets of paleomagnetic logs. All the processed samples were thermally demagnetized in 15–17 steps at 50–30^oC intervals (between 50 and 680^oC) with an MMTD-80 Thermal Demagnetizer. Remanent magnetization and magnetic orientation were measured on a 2G-755R Superconductiing Rock Magnetometer in the magnetically shielded room of the Paleomagnetic Laboratory of the Key Laboratory of western China's Environmental System (MOE), Lanzhou University.

Two components are generally distinguished in the palaeomagnetic signal, by contrasting directions and intensities. A low-temperature component (LTC) in roughly the normal polarity direction is removed gradually by thermal treatment in the interval 100–150 ^oC (but sometimes up to 200–350 ^oC). This LTC is generally interpreted as a secondary remanent magnetization characterized by a viscous superimposed direction. Upon removal of the LTC, a high-temperature component (HTC) shows relatively stable directions and linear decay in intensity toward the origin. This HTC is generally interpreted as the primary magnetization acquired during deposition. The directions of the HTC are calculated using the least-squares fitting technique (Kirschvink, 1980) for selected demagnetization data points (minimum of three, but mostly 5–10).

~~2.5. OSL dating~~

~~In order to evaluate the formation ages of T1, a single OSL sample was collected in a metal cylinder, using standard methodology, from the lower part of overbank sediments belonging to this terrace (Fig. 5). The sample was pretreated according to the method by Zhao and Li (2002) and measurement (in the Luminescence Laboratory of the Qinghai Institute of Salt Lakes, Chinese Academy of Sciences) used an automated Risø TL/OSL DA-20 reader, applying the double single-aliquot regeneration-dose procedure (Banerjee et al., 2001).~~

4~~3~~. Results

43.1. The terrace succession

A well-preserved sequence of five strath terraces was identified between the present river bed and the planation surface (Fig. 4C and D), within which the uppermost terrace is ~~a~~ newly recognized ~~terrace~~ in comparison with the previous study by Pan et al. (2005a). The term strath terrace is used here to describe an erosional terrace with only a relatively thin gravel layer, isolated vertically from the gravels of other terraces. In this terrace sequence, all treads are eroded into the Early Pleistocene lacustrine Sanmen Formation (see Fig. 4E for sedimentary characteristics). The planation surface, cut through pre-existing limestone, basin-fill sediments, and tectonic structures, is overlain by 12.5-m-thick Red Clay and a 139.5 m thick loess sequence, characterized by alternating loess (L) and palaeosol (S) units (Fig. 7). No indications of erosional disconformity between the Red Clay and the loess have been observed. Palaeosol complex S5, consisting of three sub-palaeosols, is the most prominent one within the sequence on the Chinese Loess Plateau, and is distinguished by its great thickness and dark color, being generally regarded as a marker layer (Liu, 1985). It can be discerned by field observations to occur at a depth of 107.6–115.3 m in the aeolian cover of the planation surface at Sanmenxia, which contains 32 palaeosol units (Fig. 7). ~~On the basis of this marker layer, the loess stratigraphy above this surface may be divided into 32 palaeosol units (from S32 to S1).~~ The loess deposits above the gravels of terraces T5, T4, T3, and T2 are ~130, 114, 64, and 30 m thick respectively (Fig. 7). From detailed field observations, the loess stratigraphy on these four terraces can be divided, respectively, into fifteen, nine, six, and three red palaeosol units, which can be readily correlated with the upper palaeosol units (S14 to S1) on the planation surface. The basal palaeosol units of each terrace can be shown to overlie the fluvial deposits without a significant hiatus. In the case of the planation surface and terrace T5, these pedostratigraphic correlations, based on field observations, have been further corroborated by patterns of magnetic susceptibility variation ~~and by OSL geochronology~~ (see below). The lowermost terrace has been OSL-dated to 12.7 ± 1.2 ka (HZB-2; Fig. 5).

43.2. Magnetic susceptibility ~~and OSL ages~~

~~As noted above,~~ Mmagnetic susceptibility reflects the distinction between loess

(L) and palaeosols (S), with higher values in palaeosols than in loess~~, proving to be a considerable aid in determining the loess – soil stratigraphy of the region~~ (e.g., Kukla et al., 1988; Maher and Thompson, 1991; Soreghan et al., 1997). The variation patterns of magnetic susceptibility in the loess deposits on the planation surface and uppermost terrace (T5) are closely consistent with field observations of pedostratigraphy (Fig. 7). For palaeosol complex S5 in the two studied loess covers, the magnetic susceptibility increases steeply and reaches its highest value in the middle part of this complex, suggesting a prominently developed palaeosol unit. More specifically, large amplitude fluctuations of magnetic susceptibility appear in this palaeosol complex, showing three marked peaks that correspond well with the three subsidiary divisions of this prominent S5 palaeosol. Using S5 as a marker horizon, magnetic susceptibility data were used to divide the loess sequences on the planation surface and terrace T5, respectively, into 32 (from S1 to S32, with the basal loess unit L33) and 15 (Sm–S14) established palaeosol units. The magnetic susceptibility patterns from these two loess covers are in good agreement with comparable records from the Chinese Loess Plateau (e.g., Lu et al., 1999; Pan et al., 2012). Their high magnetic susceptibility values match well with the light red palaeosol units, implying that the pedostratigraphic divisions based on field observations, as described in this paper, are reliable.

The Red Clay beneath the Quaternary loess w~~h~~as deposited~~accumulated~~ immediately on top of the planation surface. Its magnetic susceptibility gradually increases upwards, reaching its highest value at the top of the unit. Further upwards, the values decrease markedly in the overlying pedogenic carbonate nodule layer and then recover in the transitional layer (TU) between Red Clay and the overlying Quaternary loess. This pattern of magnetic susceptibility in the Red Clay obtained here concurs with magnetic susceptibility records from late Pliocene Red Clay sections on the Chinese Loess Plateau (Sun et al., 2006; Pan et al., 2011).

~~<Table 2 hereabout>~~

~~For the lowest terrace (T1), the analytical data and results from OSL dating are tabulated in Table 2. This OSL sample (Laboratory ID: HZB-2) collected from the lower part of the overbank sediments on this terrace was dated at 12.7 ± 1.2 ka (Fig. 5), consistent with emplacement of the overbank sediments of terrace T1 since the last~~

~~glacial maximum of the Late Pleistocene.~~

~~4~~3.3. Paleomagnetism

Three sets of palaeomagnetic transects, collected from the aeolian covers of the planation surface and terrace T5 at each section, show similar properties. Most samples maintain strong remanent magnetization, with clear separation of characteristic remanent magnetization (ChRM) directions (see Fig. 8 for the typical thermal demagnetization diagrams).

<Fig. 8 hereabout>

The pedostratigraphy and magnetic patterns of the aeolian covers on the planation surface and uppermost terrace (T5) are illustrated in Fig. 7. The magnetostratigraphic patterns from the two covers can be correlated with the geomagnetic polarity timescale (GPTS) of Cande and Kent (1995).

In the 152.0-m thick aeolian deposits on the planation surface, both the stratigraphic subdivision of the loess and the conformity between the Red Clay and overlying loess deposits provide a reliable indication that the chronology of the aeolian cover extends from the Pliocene to the late Pleistocene (Liu, 1985). Thus the obtained magnetozones correlate typically with the polarity intervals from Brunhes to Gauss in the geomagnetic polarity timescale. The Gauss normal-polarity chron occurs between 0.5 and 11.5 m above the planation surface and includes two reversed-polarity subchrons that pinpoint the basal age of aeolian deposits here to the Kaena and Mammoth subchrons. The Gauss–Matuyama boundary occurs in the lower part of TU, which is also the boundary between the Neogene Red Clay and Quaternary loess (Liu, 1985; Ding et al., 1990). The Olduvai normal subchron, spanning 38–30 m, occurs between S27 and L25. The Jaramillo normal subchron, extending from 74.5 to 82.0 m, is registered between S11 and L10. The Matuyama-Brunhes boundary is found at a depth of 98.0 m in L8. These paleomagnetic polarity events identified in the stratigraphy on the planation surface are in full agreement with the well-established loess and Red Clay magnetostratigraphy on the Chinese Loess Plateau (cf. Kukla and An, 1989; Rutter et al., 1991; Zhu et al., 1994; Ding et al., 1998; Pan et al., 2012). On the Loess Plateau,

since the sedimentation rate in the Red Clay (~1.5 cm/ky) was generally lower than that in the Quaternary loess (~10 cm/ky) (e.g., Vandenberghe et al., 2004), extrapolation of the prevailing accumulation rate of the Red Clay (here, ~1.1 cm/ky within the Gauss chron) below the lower boundary of the Gauss normal polarity chron is a more logical approach for dating the basal Red Clay, rather than using an accumulation rate averaged over the entire aeolian sequence (Red Clay and loess). This approach yields an estimated age of ~3.63 Ma for the onset of aeolian deposition on the planation suface.

For the ~130 m thick loess cover stacked on the uppermost terrace (T5), the Matuyama–Brunhes boundary occurs at a depth of 49.0 m and coincides with L8. The Jaramillo normal subchron, spanning from 18.0 to 28.5 m, is registered between S11 and L10. It is clear that the positions of these paleomagnetic polarity events may readily be correlated with the magnetostratigraphy derived from the aeolian cover of the planation surface. Extrapolation of the prevailing accumulation rate of the loess deposits (~10.5 cm/ky) below the lower boundary of the Jaramillo normal subchron produces an estimated age of ~1.24 Ma for the basal loess deposits lying on this terrace.

5~~4~~. Discussion

5~~4~~.1. Age determination of the fluvial terraces within the Sanmen gorge

~~It is well-known that the dating of aeolian deposits can provide an indication of the age of underlying geomorphic surfaces, particularly river terraces. In the eastern part of the Chinese Loess Plateau, it has been shown that dust-fall was persistent from late Miocene times onwards (Qiang et al., 2001; Zhao et al., 2002) and thus the accumulation of aeolian deposits can be assumed to have started immediately after the formation of the underlying landforms (e.g., Porter et al., 1992; Pan et al., 2009). In addition, I~~in most cases there is a gradual transition from terrace gravel to overbank sediments and, finally, to primary (in situ) aeolian deposits (Vandenberghe et al., 2012). Therefore, the basal age of the aeolian deposits immediately overlying the planation surface and terrace treads can be roughly equated with the formation times of the geomorphic surfaces (planation and fluvial terrace surfaces). Supplementary to the previous dating of~~In the case of the sequence in the research area,~~ terraces T4, T3,

and T2~~ were previously dated~~ by Pan et al. (2005a), to ~~ to~~ 860, 620, and 129 ka, respectively, t~~. T~~he newly recognized planation surface and uppermost terrace (T5) have now provided age estimates also (Fig. 7). Although the terrace called T5 here was previously recognized by Kong et al. (2014), its age was not determined successfully by their cosmogenic radio nuclide (CRN) study, which may be linked to the difficulty of getting reliable burial dates from river terrace deposits (Rixhon et al., 2016). In comparison, the latter authors assigned an age of 1.3 Ma to the lower sediments of terrace T4, which is older than the abandonment age of 860 ka obtained by Pan et al (2005a). According to the magnetostratigraphic analyses of the basal parts of the aeolian covers, the ages of the planation surface and terrace T5 are ~3.63 Ma and ~1.24 Ma, respectively; the latter age is close to the 1.5 – ~~-~~1.3 Ma suggested by Kong et al. (2014) for the initiation of drainage (by the Weihe River) through the Sanmen gorge.

~~The OSL age for the lower overbank sediments suggests that the lowest terrace (T1) was formed after ~12 ka.~~

~~——~~On the basis of field investigation, the tread of the uppermost terrace (T5) at Sanmenxia can be traced over an extensive area upstream and extending downstream into the inner Sanmen gorge, and can be correlated tentatively (based on height above modern river) with the uppermost terraces formed at Zhangbian, Dongcun, and Xiaolangdi (Fig. 6). This distribution~~al~~ pattern indicates that the uppermost terrace below the planation surface is generally continuous, representing the initial fluvial incision by the Yellow River within the gorge. In addition, the magnetostratigraphic record from the uppermost terrace at Kouma, downstream of the Sanmen gorge, has also been dated previously to ~1.2 Ma (Pan et al., 2005b). The temporal coincidence of the uppermost terraces upstream and downstream of this gorge suggests that the first phase of downcutting by the Yellow River from the planation surface to the level of the uppermost terrace was prior to ~1.2 Ma (again in general agreement with the previous conclusions of Kong et al. (2014)).

5~~4~~.2. Evolution of the middle to lower Yellow River catchment from~~Fluvial landscape evolution by the Yellow River from~~ basin filling to entrenchment~~excavation~~

The magnetostratigraphic record from the aeolian cover of the planation surface at Sanmenxia suggests that before 3.63 Ma the Fenwei graben (represented by the

Formatted: Indent: First line: 2 ch

Lingbao basin) had become progressively filled with the lacustrine sediments (Fig. 9AI). Geomorphic investigation along the Sanmen gorge (Fig. 5) indicates that at this time the local relief was progressively lowered to basin-fill level, eventually forming the planation surface (Fig. 9AII) that extends across the Fenwei graben and the surrounding mountain ranges (including the Xiaoshan) as was the case at the northern Tibetan Plateau (Wang et al., 2012).

<Fig. 9 hereabout>

Elsewhere, the development of low-relief landscapes ('planation surface') has been claimed as a reliable marker to indicate subsequent landscape rejuvenation, uplift and deformation (e.g., Ollier and Pain, 2000; Clark et al., 2004; Peulvast and Sales, 2004). Before and during the Pliocene, large parts of Europe, Africa, and Asia were planated, all in areas that were unaffected by plate motions, thus leading to the widespread development of low-relief landscapes (e.g., Cui et al., 1996; Danišík et al., 2006; Coltorti et al., 2007; Wagner et al., 2011; Pan et al., 2012; Vandenberghe, 2016). The comparable low-relief landscape or 'planation surface', recognized in and around the Fenwei graben and the Xiaoshan has been significantly uplifted by plate tectonic processes and subsequently ~~and~~ dissected. ~~This is a result, we suggest, of plate tectonic processes, with erosion perhaps enhanced by the strengthened of the East Asian monsoon (see above).~~ The continuation of tectonic activity after the formation of the planation level during the late Pliocene and Quaternary can be demonstrated. First, as is apparent from the geomorphic section at Sanmenxia (Fig. 5), the downthrow of the hanging-walls along the ~~indicates that~~ normal faults bounding the Lingbao basin (within the ~~older~~ graben system of the Fenwei; Fig. 9B) ~~were active ~3.63 Ma; the downthrow in their hanging walls~~ disrupted the ~~older~~ 'planation surface', which itself became uplifted in the Xiaoshan area. Second, seismic data also~~analysis~~ indicate~~s~~ that the normal faults bounding the Lingbao basin have remained active during the Quaternary (Li et al., 2015). The ~~In this case, the subsequent~~ evolution of this active basin was probably independent of the rest of the southern Shanxi rift. As the Xiaoshan mountains grew higher, the ancestral fluvial system that drained their~~its~~ eastern front ~~,~~ began to cut headward, toward the west (Wang et al., 2001).

The sedimentary record in the North Pacific indeed shows that dust deposition

increased quite rapidly, by an order of magnitude, at 3.6 Ma (Rea, et al., 1998), which may have been associated with the uplift of the Tibetan Plateau and the cooling of the northern hemisphere. Continuous aeolian deposition in the present study region also began by this time, resulting in accumulation on the 'planation surface' (our basal age). After this time, this inner sub-basin of the Fenwei graben, which previously drained internally, became filled with fluvio-lacustrine sediments (the Sanmen Formation, illustrated in Fig. 4E) with a paleolake eventually covering much of the graben (Liu, 2004). This lake was then drained and the Sanmen gorge formed, initiating external drainage and linkage to the Yellow River system.

We suggest that the remarkable transition of the Fenwei graben, from filling to excavation (incision), was thus associated with the establishment of external drainage and the formation of the Sanmen gorge. ~~Our data (Fig. 9CI) imply that gorge incision started between 3.63 (the age of the planation surface) and 1.24 Ma (the age of the highest terrace, which is below the top of the gorge sides), broadly confirming the findings of Kong et al. (2014).~~ The Xiaoshan barrier may have been breached by lake spillover as the ancestral fluvial system at its eastern front cut headward towards the Lingbao basin (Fig. 9C, I). Subsequently, following the emptying of the lake, fluvial incision into the sediments of the Sanmen Formation began (Fig. 9CII). The geomorphic evidence indeed suggests that this drainage integration was associated with fluvial downcutting, from the 'planation surface' down to the level of the uppermost terrace (T5). The approximately synchronous development of this terrace both within the Sanmen gorge and further downstream at Kouma (see above), with dates of ~1.24 Ma and 1.2 Ma (respectively), indicates that the modern Yellow River had been established by this time and~~.~~ ~~s~~Subsequently became entrenched~~ment by the Yellow River progressively created the present Sanmen gorge~~ (Fig. 9D). The formation of a river terrace staircase within the Fenwei graben is notable, implying that the graben interior is uplifting (a requirement for terrace formation), albeit at a slower rate than the crust outside the faulted interior of the system (cf. Gao et al., 2016).

The initial development of the Sanmen gorge was thus an important event, since it marked the initiation of the eastward-flowing drainage of the Yellow River. Once this gorge had begun to form, terrigenous sediments could be transported from the interior of the Tibetan Plateau, in the upper reaches of the Yellow River, to the Bohai Gulf. Although~~s already noted,~~ loess began to accumulate in the present study region

Formatted: Font: Times New Roman

at significant rates by ~3.6 Ma. ~~(Rea et al., 1998). However,~~ terrigenous sedimentation rates on the North China Plain and in the Bohai Gulf did not show dramatic increases until ~1.0 Ma (Xiao et al., 2008; Yao et al., 2010, 2012), in all probability in response to the formation of the Sanmen gorge. As Nie et al. (2015) have suggested, the majority of the sediment liberated by the dissection of the 'planation surface' from the middle and upper Yellow River basins was probably stored on the Chinese Loess Plateau before the through-going Yellow River drainage system was formed.

~~Similar sequences of events, whereby ancestral lake basins were disrupted and replaced by fluvial drainage, are also recognized in other continental interior regions worldwide. For example, the history of integration of the upper reaches of the modern River Euphrates (in the eastern Anatolian Plateau) with the rest of its catchment, starting in the Mid-Pleistocene and associated with the disruption of paleolake basins, as investigated by Seyrek et al. (2008), Westaway et al. (2008), and Demir et al. (2009). Regional uplift of the eastern Anatolian Plateau and active faulting both played a part in this sequence of events. Another example, documented by Westaway et al. (2009), was the integration of the modern Rio Grande River in the central southern USA. In that example the upper reaches of the ancestral river system drained into a paleolake in the Rio Grande Rift, an actively-developing graben; however, faster regional uplift following the Mid-Pleistocene Revolution resulted in disruption of this lake basin and the initiation of fluvial entrenchment, marked by dated river terraces, into its former interior. Numerous other examples of 'inverted' Late Cenozoic fluvio-lacustrine basins could be documented, including many reported by earlier FLAG research (e.g., Matoshko et al., 2004; Bridgland and Westaway, 2014) and in the present issue (Bridgland et al., 2016; Cunha et al., 2016; Maddy et al., 2016).~~

The formation of the Sanmen Gorge, which enabled through drainage from the upper Yellow River to the Bohai Gulf, would appear to have been the last~~final~~ in a series of linkage events joining inland basins. This progressive drainage linkage can now be envisaged to have occurred in sequence from upstream to downstream (contra Molnar, 2004), perhaps by means of repeated basin overflow in response to progressive basin filling coupled with increasing precipitation from the strengthening Asian Monsoon. The occurrence of this final eastern completion of the through-flowing Yellow River can also be demonstrated by the change in the type of zircon~~s~~ grains in the thick perched sedimentary sequence at Liujiahou (close to our

site at Sanmenxia) reported by Kong et al. (2014), and called T5 by them. Zircon in the lower sediments here were of more local origin, whereas those from a sample high in the sequence (like those from later terrace sediments) were from upstream in the Yellow River, suggesting that basins upstream had been joined to form a through-flowing system by the time these uppermost sediments were deposited, just before incision by the newly-formed river and the development of the lower terrace staircase.

54.3. Wider comparisons

Similar sequences of events, whereby ancestral lake basins were disrupted and replaced by fluvial drainage, are also recognized in other continental interior regions worldwide. For example, the history of integration of the upper reaches of the modern River Euphrates (in the eastern Anatolian Plateau) with the rest of its catchment, starting in the Mid-Pleistocene and associated with the disruption of paleolake basins, as investigated by Seyrek et al. (2008), Westaway et al. (2008), and Demir et al. (2009). Regional uplift of the eastern Anatolian Plateau and active faulting both played a part in this sequence of events. Another example, documented by Westaway et al. (2009), was the integration of the modern Rio Grande River in the central-southern USA. In that example the upper reaches of the ancestral river system drained into a paleolake in the Rio Grande Rift, an actively-developing graben; however, faster regional uplift following the Mid-Pleistocene Revolution resulted in disruption of this lake basin and the initiation of fluvial entrenchment, marked by dated river terraces, into its former interior. Numerous other examples of 'inverted' Late Cenozoic fluvio-lacustrine basins could be documented, including many reported by earlier FLAG research (e.g., Matoshko et al., 2004; Bridgland and Westaway, 2014) and in the present issue (Bridgland et al., 2016; Cunha et al., 2016; Maddy et al., 2016).

Attempts have recently been made to integrate onshore datasets indicating rates of erosion and offshore datasets indicating rates of deposition (e.g., Herman et al., 2013; Herman and Champagnac, 2016). It has been argued on the basis of increases in offshore sedimentation rates that accordingly terrestrial erosion rates increased (e.g., Zhang et al., 2001; Molnar, 2004). However, others have rejected the idea that erosion rates have increased in the Late Cenozoic (e.g., Willenbring and von Blanckenburg,

2010; Sadler and Jerolmack, 2015; Willenbring and Jerolmack, 2016). It has been shown here that the Yellow River and other major rivers only became integrated with their present catchment geometries in the relatively recent geological past, such that, beforehand, the products of erosion throughout much of these catchments were trapped in inland depocentresers and were thus unable to reach the sea. This has to be considered as an important complicating factor in attempting comparison of global datasets of Late Cenozoic onshore erosion and offshore deposition.

~~An interesting point of comparison with other regions concerns the recognition, within the Fenwei graben, of a river terrace staircase (Fig. 9D), thus implying that the graben interior is uplifting (a requirement for terrace formation), albeit at a slower rate than the crust outside the faulted interior of the system. Absolute uplift has also been recognized within the interiors of onshore grabens flanking the Aegean Sea (e.g., Westaway, 1993a), thus superseding the former paradigm that hanging-wall localities are always subsiding (cf. Jackson and McKenzie, 1983). Uplift has also been recognized in graben interiors or normal fault hanging-walls in many other regions, including southern Italy (Westaway, 1993; Westaway and Bridgland, 2007), Bulgaria (Westaway, 2006), central-southern Turkey (Seyrek et al., 2014), and the aforementioned Rio Grande Rift in the central-southern USA (Westaway et al., 2009).~~

Formatted: Indent: First line: 0 cm

65. Conclusions

Downcutting by the Yellow River into the Xiaoshan range, below a planation surface dated to ~3.63 Ma, has resulted in the formation of the Sanmen gorge. On the basis of detailed field investigation, a new and uppermost Yellow River terrace, T5, has been recognized along the gorge. As a result, a sedimentary and geomorphic archive of five terraces was formed, in addition to the above-mentioned planation surface. Magnetostratigraphic records from the aeolian deposits accumulated on top of these surfaces provide a geochronological framework for this archive. The ages of the planation surface (P) and terraces T5, T4, T3, T2, and T1 have beenwere determined at ~3.63 Ma, ~1.24 Ma, ~0.86 Ma, ~0.62 Ma, ~129 ka, and ~12 ka, respectively. Thus, the formation ages of the planation surface and uppermost terrace suggest that this gorge was entrenched primarily between 3.63 and 1.24 Ma. At the same time the landscape of the Fenwei region switched from basin filling to excavation (‘basin inversion’) enabling the formation of a series of terraces within the graben.; ~~which~~

~~could be termed 'basin inversion'.~~ Before the start of entrenchment of the Sanmen gorge, the products of erosion in the modern upper catchment of the Yellow River were 'trapped' inland and, therefore, unable to reach the sea. The dramatic increase in deposition rates in the Bohai Gulf, at the mouth of the modern Yellow River, at ~1.0 Ma, resulted from the integration of the Yellow River catchment following the initiation of drainage through Sanmen gorge and does not imply an increase in erosion rates at that time.

Acknowledgements

We are grateful to Xiaopeng Liu, Jian Zhang, and Prof. Qingyu Guan for assistance with the field sampling and laboratory analyses. The comments by Prof. Frank J. Pazzaglia, an anonymous referee, and the special issue editor, Stéphane Cordier, have led to considerable improvements and are gratefully acknowledged. This research is financially supported by the National Natural Science Foundation of China (Grant no. 41401001, 41571003), the Key Project of the Major Research Plan of the NSFC (Grant no. 91125008), the National Basic Research Program of China (2011CB403301), and the Fundamental Research Funds for the Central Universities.

References

AFSOM, 1988. Active fault system around Ordos Massif. Seismological Press, Beijing, pp. 77-136 (in Chinese).

An, Z., Kutzbach, J.E., Prell, W.L., Porter, S.C., 2001. Evolution of Asian monsoon and phased uplift of the Himalayan-Tibetan Plateau since Late Miocene times. Nature 411, 62-66.

~~Banerjee, D., Murray, A.S., Bøtter-Jensen, L., Lang, A., 2001. Equivalent dose estimation using a single aliquot of polymineral fine grains. Radiation Measurements 33, 73-94.~~

Bridgland, D.R., 2000. River terrace systems in north-west Europe: an archive of environmental change, uplift and early human occupation. Quaternary Science Reviews 19, 1293-1303.

Bridgland, D.R., Westaway, R., 2008. Climatically controlled river terrace staircases: A worldwide Quaternary phenomenon. Geomorphology 98, 285-315.

Bridgland, D.R., Westaway, R., Abou Romieh, M., Candy, I., Daoud, M., Demir, T., Galiatsatos, N., Schreve, D., Seyrek, A., Shaw, A., White, T., Whittaker, J., 2012. The River Orontes in Syria and Turkey: Downstream variation of fluvial archives in different crustal blocks. Geomorphology 165-166, 25-49.

Bridgland, D.R., Westaway, R., 2014. Quaternary fluvial archives and landscape evolution: a global synthesis. Proceedings of the Geologists' Association 125, 600-629.

Bridgland, D.R., Demir, T., Seyrek, A., Abou Romieh, M., Daoud, M., Westaway, R., 2016. River terrace development in the NE Mediterranean region (Syria and Turkey): patterns in relation to crustal type. Quaternary Science Reviews.

Bull, W.B., 1990. Stream-terrace genesis: implication for soil development. Geomorphology 3, 351-367.

Cande, S.C., Kent, D.V., 1995. Revised calibration of the geomagnetic polarity timescale for the Late Cretaceous and Cenozoic. Journal of Geophysical Research 100, 6093-6095.

Cheng, S., Deng, Q., Zhou, S., Yang, G., 2002. Strath terraces of Jinshaan Canyon, Yellow River, and Quaternary tectonic movements of the Ordos Plateau, north China. Terra Nova 14, 215-224.

Clark, K.M., Schoenbohm, M.L., Royden, H.L., Whipple, X.K., Burchfiel, C.B., Zhang, X., Tang, W., Wang, E., Chen, L., 2004. Surface uplift, tectonics, and erosion of eastern Tibet from large-scale drainage patterns. Tectonics 23, TC1006, doi:10.1029/2002TC001402.

Clift, D.P., 2006. Controls on the erosion of Cenozoic Asia and the flux of clastic sediment to the ocean. Earth and Planetary Science Letters 241, 571-580.

Coltorti, M., Dramis, F., Ollier, D.C., 2007. Planation surfaces in Northern Ethiopia. Geomorphology 89, 287-296.

Craddock, H.W., Kirby, E., Harkins, W.N., Zhang, H., Shi, X., Liu, J., 2010. Rapid fluvial incision along the Yellow River during headward basin integration. Nature Geoscience 3, 209-213.

Cui, Z., Gao, Q., Liu, G., Pan, B., Chen, H., 1996. Planation surface, palaeokarst and uplift of Xizang (Tibet) Plateau. Science in China 39, 391-400.

Cunha, P.P., Martins, A.A., Buylaert, J.P., Murray, A.S., Raposo, L., Mozzi, P., Stokes, M., 2016. New data on the chronology of the Vale do Forno sedimentary sequence (Lower Tejo River terrace staircase) and its relevance as a fluvial archive of the Middle Pleistocene in western Iberia. Quaternary Science Reviews. http://dx.doi.org/10.1016/j.quascirev.2016.11.001.

Danišík, M., Kuhlemann, J., Dunkl, I., Székely, B., Frisch, W., 2006. Significance of high-elevated planation surfaces in interpreting thermotectonic evolution of the mountains. Goldschmidt Conference Abstracts A126.

Demir, T., Seyrek, A., Guillou, H., Scaillet, S., Westaway, R., Bridgland, D.R., 2009. Preservation by basalt of a staircase of latest Pliocene terraces of the River Murat in eastern Turkey: evidence for rapid uplift of the eastern Anatolian Plateau. Global and Planetary Change 68, 254-269.

Ding, Z., Liu, T. S., Liu, X. M., Chen, M. Y., An, Z. S., 1990. Thirty-seven climatic cycles in the last 2.5 Ma. Chinese Science Bulletin. 34, 1494-1496.

Ding, Z., Sun, J.M., Yang, S.L., Liu, T.S., 1998. Preliminary magnetostratigraphy of a thick eolian red clay-loess sequence at Lingtai, the Chinese Loess Plateau. Geophysical Research Letters. 25, 1225-1228.

Ding, Z., Derbyshire, E., Yang, S., Yu, Z., Xiong, S., Liu, T., 2002. Stacked 2.6-Ma grain size record from the Chinese loess based on five sections and correlation with the deep-sea $\delta^{18}O$ record. Paleoceanography 17, 1033-1053.

Dong, Y., Zhang, G., Neubauer, F., Liu, X., Genser, J., Hauzenberger, C., 2011. Tectonic evolution of the Qinling orogen, China: Review and synthesis. Journal of Asian Earth Sciences 41, 213-237.

Fan, D., Li, C., 2008. Timing of the Yangtze initiation during the Tibetan Plateau throughout to the East China Sea: A review. Front Earth Science China 2, 302-313.

Gao, H., Li, Z., Ji, Y., Pan, B., Liu, X., 2016. Climatic and tectonic controls on strath terraces along the upper Weihe River in central China. Quaternary Research 86, 326-334.

Geng X., 1981. Marine transgressions and regressions in East China since Late Pleistocene epoch. Acta Oceanologica Sinica 3, 114-130 (in Chinese, with English

abstract).

Guo, Y., Zhang, J., Qiu, W., Hu, G., Zhuang, M., Zhou, L., 2012. Luminescence dating of the Yellow River terraces in the Hukou area, China. Quaternary Geochronology 10, 129-135.

He, P., Liu, L., Yu, Q., 1984. The age of the Sanmen series and the evolution of its depositional environment discussed in the light of the Dongpogou section in the Sanmen gorge area. Geological Reviews 30, 161-169 (in Chinese, with English abstract).

Herman, F., Champagnac, J.-D., 2016. Plio-Pleistocene increase of erosion rates in mountain belts in response to climate change. Terra Nova, 28, 2–10.

Herman, F., Seward, D., Valla, P.G., Carter, A., Kohn, B., Willett, S.D., Ehlers, T.A., 2013. Worldwide acceleration of mountain erosion under a cooling climate. Nature, 504, 423–426.

~~Hu, Z.B., Pan, B.T., Guo, L.Y., Vandenberghe, J., Liu, X., Wang, J., Fan, Y., Mao, J., Gao, H., Hu, X., 2016. Rapid fluvial incision and headward erosion by the Yellow River along the Jinshaan gorge during the past 1.2 Ma as a result of tectonic extension. Quaternary Science Reviews 133, 1-14.~~

Huang, Z., Xu, M., Wang, L., Mi, N., Yu, D., Li, H., 2008. Shear wave splitting in the southern margin of the Ordos Block north China. Geophysical Research Letters 35, L19301. http://dx.doi.org/10.1029/2008GL035188.

~~Jackson, J., McKenzie, D., 1983. The geometrical evolution of normal fault systems. Journal of Structural Geology 5, 471-482.~~

Ji, J., Zheng, H., Li, S., Huang, X., 2006. The terraces of the Huanghe River in Pinglu County, Shanxi Province and their relationship with the disappearance of the Sanmen palaeolake and the formation of the Huanghe River. Quaternary Sciences 26, 665-672 (in Chinese, with English abstract).

Jiang, F., Fu, J., Wang, S., Sun, D., Zhao, Z., 2007. Formation of the Yellow River, inferred from loess-palaeosol sequence in Mangshan and lacustrine sediments in Sanmen Gorge, China. Quaternary International 175, 62-70.

Kirschvink, J.L., 1980. The least-squares line and plane and the analysis of palaeomagnetic data. Geophysical Journal International 62, 699-718.

Kong, P., Jia, J., Zheng, Y., 2014. Time constraints for the Yellow River traversing the Sanmen Gorge. Geochemistry, Geophysics, Geosystems 15, 395-407.

Kukla, G., An, Z.S., 1989. Loess stratigraphy in central China. Palaeogeography, Palaeoclimatology, Palaeoecology. 72, 203-225.

Kukla, G., Heller, F., Liu, M., Xu, C., Liu, S., An, S., 1988. Pleistocene climates in China dated by magnetic susceptibility. Geology 16, 811-814.

Li, J., 1991. The environmental effects of the uplift of the Qinghai-Xizang Plateau. Quaternary Science Reviews 10, 479-483.

Li, B., Sørensen, M.B., Atakan, K., 2015. Coulomb stress evolution in the Shanxi rift system, North China, since 1303 associated with coseismic, post-seismic and interseismic deformation. Geophysical Journal International 203, 1642-1664.

Lin, A.M., Yang, Z.Y., Sun, Z.M., Yang, T.S., 2001. How and when did the Yellow River develop its square bend? Geology 29, 951-954.

Liu, H., 2004. Formation and evolution of the Weihe River basin and uplift of the eastern Qinling Mountains, Ph.D. thesis, The Northeast University, Xian, China.

Liu, J., Zhang, P., Lease, R.O., Zheng, D., Wan, J., Wang, W., Zhang, H., 2013. Eocene onset and late Miocene acceleration of Cenozoic intracontinental extension in the North Qinling range-Weihe graben: Insights from apatite fission track thermochronology. Tectonophysics 584, 281-296.

Liu S., Li, G., Li, Y., Jin, J., 1988. The sedimentary characteristics of the North China plain as an indicator for the formation and evolution of the Yellow River. Henan Geology 6, 20-24 (in Chinese).

Liu, T., 1985. Loess and the Environment. China Ocean Press, Beijing, pp. 31-147.

Liu, X., Chen, B., 2000. Climatic warming in the Tibetan Plateau during the recent decades. International Journal of Climatology 20, 1729-1742.

Lu, H., Liu, X., Zhang, F., An, Z., Dodson, J., 1999. Astronomical calibration of loess-palaeosol deposits at Luochuan, central Chinese Loess Plateau. Palaeogeography, Palaeoclimatology, Palaeoecology 154, 237-246.

Maddy, D., Veldkamp, A., Demir, T., van Gorp, W., Wijbrans, J.R., van Hinsbergen, D.J.J., Dekkers, M.J., Schreve, D., Schoorl, J.M., Scaife, R., Stemerdink, C., van der Schriek, T., Bridgland, D.R., Aytaç, A.S., 2016. The Gediz River fluvial archive: a benchmark for Quaternary research in Western Anatolia. Quaternary Science Reviews. http://dx.doi.org/10.1016/j.quascirev.2016.07.031.

Maher, B.A., Thompson, R., 1991. Mineral magnetic record of the Chinese loess and palaeosols. Geology 19, 3-6.

Matoshko, A., Gozhik, P., Danukalova, G., 2004. Key Late Cenozoic fluvial archives of eastern Europe: the Dniester, Dnieper, Don and Volga. Proceedings of the Geologists' Association 115, 141-173.

Miao, X., Lu, H., Li, Z., Cao, G., 2008. Paleocurrent and fabric analyses of the imbricated fluvial gravel deposits in Huangshui Valley, the northeastern Tibetan Plateau, China. Geomorphology. 99, 433-442.

Molnar, P., 2004. Late Cenozoic increase in accumulation rates of terrestrial sediment: how might climate change have affected erosion rates? Annu. Rev. Earth Planet. Sci.

32, 67–89.

Molnar, P., England, P., Martinod, J., 1993. Mantle dynamics, uplift of Tibetan Plateau, and the Indian Monsoon. Reviews of Geophysics 31, 357-396.

~~Molnar, P., Boos, R.W., Battisti, S.D., 2010. Orographic controls on climate and paleoclimate of Asia: Thermal and mechanical roles for the Tibetan Plateau. Annu. Rev. Earth Planet. Sci. 38, 77-102.~~

Nie, J., Stevens, T., Rittner, M., Stockli, D., Garzanti, E., Limonta, M., Bird, A., Ando, S., Vermeesch, P., Saylor, J., Lu, H., Breecker, D., Hu, X., Liu, S., Resentini, A., Vezzoli, G., Peng, W., Carter, A., Ji, S., Pan, B., 2015. Loess Plateau storage of Northeastern Tibetan Plateau-derived Yellow River sediment. Nature Communications 6, 1-8.

Ollier, C.D., Pain, C.F., 2000. The Origin of Mountains. Routledge, London.

Pan, B., Li, J., Chen, F., 1995. The Qinghai-Tibetan Plateau: Driver and amplifier of the global climate changes. I The characteristics of climate changes in Cenozoic. Journal of Lanzhou University (Natural Science Edition) 31, 120-128 (in Chinese, with English abstract).

Pan, B.T., Burbank, D., Wang, Y.X., Wu, G.J., Li, J.J., Guan, Q.Y., 2003. A 900 k.y. record of strath terrace formation during glacial-interglacial transitions in northwest China. Geology 32, 957-960.

Pan, B.T., Wang, J.P., Gao, H.S., Chen, Y.Y., Li, J.J., Liu, X.F., 2005a. Terrace dating as an archive of the run-through of the Sanmen Gorge. Progress in Natural Science. 15, 1096-1103.

Pan, B.T., Wang, J.P., Gao, H.S., Guan, Q.Y., Wang, Y., Su, H., Li, B.Y., Li, J.J., 2005b. Paleomagnetic dating of the topmost terrace in Kouma, Henan and its indication to the Yellow River's running through Sanmen Gorges. Chinese Science Bulletin. 50, 657-664.

Pan, B., Su, H., Hu, Z., Hu, X., Gao, H., Li, J., Kirby, E., 2009. Evaluating the role of climate and tectonics during non-steady incision of the Yellow River: evidence from a 1.24 Ma terrace record near Lanzhou, China. Quaternary Science Reviews 28, 3281-3290.

Pan, B.T., Hu, Z.B., Wang, J.P., Vandenberghe, J., Hu, X.F., 2011. A magnetostratigraphic record of landscape development in the eastern Ordos Plateau, China: Transition from Late Miocene and Early Pliocene stacked sedimentation to Late Pliocene and Quaternary uplift and incision by the Yellow River. Geomorphology 125, 225-238.

Pan, B.T., Hu, Z.B., Wang, J.P., Vandenberghe, J., Hu, X.F., Wen, Y.H., Li, Q., Cao, B., 2012. The approximate age of the planation surface and the incision of the Yellow River. Palaeogeography, Palaeoclimatology, Palaeoecology 356-357, 54-61.

~~Pan, G., Wang, L., Li, R., Yuan, S., Ji, W., Yin, F., Zhang, W., Wang, B., 2012. Tectonic evolution of the Qinghai-Tibet Plateau. Journal of Asian Earth Sciences 53, 3-14.~~

Perrineau, A., van der Woerd, J., Gaudemer, Y., Jing, Z., Pik, R., Tapponnier, P., Thuizat, R., Zheng, R., 2011. Incision rate of the Yellow River in Northeastern Tibet constrained by ^{10}Be and ^{26}Al cosmogenic isotope dating of fluvial terraces: implications for catchment evolution and plateau building. In: Gloaguen, R., Ratschbacher, L. (Eds.), Growth and Collapse of the Tibetan Plateau. Special Publications of the Geological Society, London 353, 189-219.

Peulvast, J.P., Sales, V., 2004. Stepped surfaces and palaeolandforms in the northern Brazilian <Nordeste>: constraints on models of morphotectonic evolution. Geomorphology 62, 89-122.

Potter, P.E., 1978. Significance and origin of big rivers. Journal of Geology 86, 13–33.

~~Porter, S.C., An, Z., Zheng, H., 1992. Cyclic Quaternary alleviation and terracing in a~~

~~nonglaciated drainage basin on the north flank of the Qinling Shan, central China. Quaternary Research 38, 157-169.~~

Powell, C., Conaghan, P.J., 1973. Plate tectonics and the Himalayas. Earth and Planetary Science Letters 20, 1-12.

Prins, M.A., Zheng, H.B., Beets, K., Troelstra, S., Bacon, P., Kamerling, I., Wester, W., Konert, M., Huang, X.T., Wang, K.E., Vandenberghe, J., 2009. Dust supply from river floodplains: the case of the lower Huang He (Yellow River) recorded in loess-palaeosol sequence from the Mangshan Plateau. Journal of Quaternary Science 24, 75-84.

~~Qiang, X.K., Li, Z.X., Powell, C.McA., Zheng, H.B., 2001. Magnetostratigraphic record of the Late Miocene onset of the East Asian monsoon, and Pliocene uplift of northern Tibet. Earth and Planetary Science Letters 187, 83-93.~~

Rea, D., Snoeckx, H., Joseph, H.L., 1998. Late Cenozoic eolian deposition in the North Pacific: Asian drying, Tibetan uplift, and cooling of the northern hemisphere. Paleoceanography 13, 215-224.

Rixhon, G., Briant, R.M., Cordier, S., Duval, M., Jones, A., Scholz, D., 2016. Revealing the pace of river landscape evolution during the Quaternary: recent developments in numerical dating methods. Quaternary Science Reviews. http://dx.doi.org/10.1016/j.quascirev.2016.08.016

~~Royden, H.L., Burchfiel, C.B., van der Hilst, D.R., 2008. The geological evolution of the Tibetan Plateau. Science 1054-1058.~~

~~Ruddiman, W.F., Kutzbach, J.E., 1989. Forcing of Late Cenozoic Northern Hemisphere climate by plateau uplift in Southern Asia and the American West. Journal of Geophysical Research 94, 18,409-18,427.~~

Rutter, N.W., Ding, Z.L., Evans, M.E., Liu, T.S., 1991. Baoji-type pedostratigraphic section, Loess Plateau, north-central China. Quaternary Science Review. 10, 1-22.

Formatted: Justified, Line spacing: 1.5 lines, Adjust space between Latin and Asian text, Adjust space between Asian text and numbers

Formatted: Font: (Default) Times New Roman

Formatted: Font: (Default) Times New Roman

Formatted: Font: (Default) Times New Roman

Sadler, P.M., Jerolmack, D.J., 2015. Scaling laws for aggradation, denudation and progradation rates: the case for time-scale invariance at sediment sources and sinks. Geological Society, London, Special Publications, 404, 69–88.

Saito, Y., Yang, Z., Hori, K., 2001. The Huanghe (Yellow River) and Changjiang (Yangtze River) deltas: a review on their characteristics, evolution and sediment discharge during the Holocene. Geomorphology 41, 219-231.

Schumm, S.A., Dumont, J.F., Holbrook, J.M., 2000. Active tectonics and alluvial river. Cambridge University Press, Cambridge, UK, pp. 375-376.

Seyrek, A., Westaway, R., Pringle, M., Yurtmen, S., Demir, T., Rowbotham, G., 2008. Timing of the Quaternary Elazığ volcanism, eastern Turkey, and its significance for constraining landscape evolution and surface uplift. Turkish Journal of Earth Sciences 17, 497-541.

~~Seyrek, A., Demir, T., Westaway, R., Guillou, H., Scaillet, S., White, S.T., Bridgland, D., 2014. The kinematics of central-southern Turkey and northwest Syria revisited. Tectonophysics 618, 35-66.~~

Soreghan, G.S., Elmore, R.D., Katz, B., Cogoini, M., Banerjee, S., 1997. Pedogenically enhanced magnetic susceptibility variations preserved in Paleozoic loessite. Geology 25, 1003-1006.

Stokes, M., 2008. Plio-Pleistocene drainage development in an inverted sedimentary basin: Vera basin, Betic Cordillera, SE Spain. Geomorphology 100, 193-211.

Sun, Y., Clemens, C. S., An, Z., Yu, Z., 2006. Astronomical timescale and palaeoclimatic implication of stacked 3.6-Myr monsoon records from the Chinese Loess Plateau. Quaternary Science Reviews 25, 33-48.

Tapponnier, P., Xu, Z., Roger, F., Meyer, B., Arnaud, N., Wittlinger, G., Yang, J., 2001. Oblique stepwise rise and growth of the Tibet Plateau. Science 294, 1671-1677.

Vandenberghe, J., Lu, H. Y., Sun, D. H., Huissteden, J., Konert, M., 2004. The late Miocene and Pliocene climate in East Asia as recorded by grain size and magnetic susceptibility of the Red Clay deposits (Chinese Loess Plateau). Palaeogeography, Palaeoclimatology, Palaeoecology. 204, 239-255.

Vandenberghe, J., Wang, X., Lu, H., 2011. Differential impact of small-scaled tectonic movements on fluvial morphology and sedimentology (the Huang Shui catchment, NE Tibet Plateau). Geomorphology 134, 171-185.

Vandenberghe, J., de Moor, J.W. J., Spanjaard, G., 2012. Natural change and human impact in a present-day fluvial catchment: The Geul River, southern Netherlands. Geomorphology 159-160, 1-14.

Vandenberghe, J., 2016. From planation surfaces to river valleys. BSGLg 67, 93-106.

Veldkamp, A., van Dijke, J. J., 2000. Simulating internal and external controls on fluvial terrace stratigraphy: a qualitative comparison with the Mass record. Geomorphology 33, 225-236.

Wagner, T., Fritz, H., Stüwe, K., Nestroy, O., Rodnight, H., Hellstrom, J., Benischke, R., 2011. Correlations of cave levels, stream terraces and planation surfaces along the River Mur-Timing of landscape evolution along the eastern margin of the Alps. Geomorphology 134, 62-78.

Wang, S., Wu, X., Zhang, K., Jiang, F., Xue, B., Tong, G., Tian, G., 2001. Sedimentary records of environmental evolution in the Sanmen Lake Basin and the Yellow River running through the Sanmenxia Gorge eastward into the sea. Science in China 31, 585-608.

Wang, X., Lu, H., Vandenberghe, J., Zheng, S., van Balen, R., 2012. Late Miocene uplift of the NE Tibetan Plateau inferred from basin filling, planation and fluvial terraces in the Huang Shui catchment. Global and Planetary Change 88-89, 10-19.

Formatted: Dutch (Netherlands)

~~Westaway, R., 1993. Quaternary uplift of southern Italy. Journal of Geophysical Research 98, 21741-21772.~~

~~Westaway, R., 2006. Late Cenozoic extension in southest Bulgaria: a synthesis. In: Robertson, A.H.F., Mountrakis, D. (Eds.), Tectonic Development of the Eastern Mediterranean Region. Special Publication, vol. 260. Geological Society, London, pp. 557-590.~~

Westaway, R., 2009. Active crustal deformation beyond the SE margin of the Tibetan Plateau: Constraints from the evolution of fluvial systems. Global and Planetary Change 68, 395-417.

~~Westaway, R., Bridgland, D.R., 2007. Late Cenozoic uplift of southern Italy deduced from fluvial and marine sediments: coupling between surface processes and lower crustal flow. Quaternary International 175, 86-124.~~

Westaway, R., Demir, T., Seyrek, A., 2008. Geometry of the Turkey-Arabia and Africa-Arabia plate boundaries in the latest Miocene to Mid-Pliocene: the role of the Malatya-Ovacık Fault Zone in eastern Turkey. eEarth, 3, 27-35.

Westaway, R., Bridgland, D.R., Sinha, R., Demir, T., 2009. Fluvial sequences as evidence for landscape and climatic evolution in the Late Cenozoic: A synthesis of data from IGCP 518. Global and Planetary Change 68, 237-253.

~~White, T.L., Lister, S.G., 2012. The collision of India with Asia. Journal of Geodynamics 56-57, 7-17.~~

Willenbring, J.K., Jerolmack, D.J., 2016. The null hypothesis: globally steady rates of erosion, weathering fluxes and shelf sediment accumulation during Late Cenozoic mountain uplift and glaciation. Terra Nova 28, 11–18.

Willenbring, J.K., von Blanckenburg, F., 2010. Long-term stability of global erosion rates and weathering during late-Cenozoic cooling. Nature 465, 211-214.

Wu, C., Xu, Q., Yang, X., 2000. Ancient drainage system of the Yellow River on North China Plain. Journal of Geomechanics 6, 1-9 (in Chinese, with English abstract).

Xia, D., Wu, S., Yu, Z., 1993. Changes of the Yellow River since the last glacial age. Marine Geology & Quaternary Geology 13, 83-88 (in Chinese, with English abstract).

Xiao, G., Guo, Z., Chen, Y., Yao, Z., Shao, Y., Wang, X., Hao, Q., Lu, Y., 2008. Magnetostratigraphy of BZ_1 borehole in west coast of Bohai bay, northern China. Quaternary Sciences 28, 909-916 (in Chinese, with English abstract).

Xue, D., 1996. A humble option of the formed age for the eastern section of the Yellow River. Henan Geology 14, 110-112 (in Chinese, with English abstract).

Yang, H., Chen, X., 1985. Quaternary transgressions, eustatic changes and shifting of shoreling in East China. Marine Geology & Quaternary Geology 5, 59-80 (in Chinese, with English abstract).

Yang, S., Cai, J., Li, C., Deng, B., 2001. New discussion about the run-through time of the Yellow River. Marine Geology & Quaternary Geolgoy 21, 15-20 (in Chinese, with English abstract).

Yao, Z., Xiao, G., Wu, H., Liu, W., Chen, Y., 2010. Plio-Pleistocene vegetation changes in the North China Plain: Magnetostratigraphy, oxygen and carbon isotopic composition of pedogenic carbonates. Palaeogeography, Palaeoclimatology, Palaeoecology 297, 502-510.

Yao, Z., Guo, Z., Xiao, G., Wang, Q., Shi, X., Wang, X., 2012. Sedimentary history of the western Bohai coastal plain since the late Pliocene: Implications on tectonic, climatic and sea-level changes. Journal of Asian Earth Sciences 54-55, 192-202.

Yu, H., 1999. Ages of the Yellow River delta in shelf regions of the Yellow sea and the Bohai sea. Journal of Geomechanics 5, 80-88 (in Chinese, with English abstract).

Yuan, Y., Hu, S., Wang, H., Sun, F., 2007. Meso-Cenozoic tectonothermal evolution of Ordos Basin, central China: Insight from newly acquired vitrinite reflectance data and a revision of existing paleothermal indicator data. Journal of Geodynamics 44, 33-46.

Yue, L., Zhang, Y., Wang, J., Deng, X., Zhang, L., 1999. Magnetostratigraphic sequence of continental deposits in Northern China since 5.3 Ma. Geological Reviews 45, 444-448 (in Chinese, with English abstract).

Zhang, J., Qiu, W., Wang, X., Hu, G., Li, R., Zhou, L., 2010. Optical dating of a hyperconcentrated flow deposit on a Yellow River terrace in Hukou, Shaanxi, China. Quaternary Geochronology 5, 194-199.

Zhang, P., Molnar, P., Downs, W.R., 2001. Increased sedimentation rates and grain sizes 2-4 Myr ago due to the influence of climate change on erosion rates. Nature 410, 891–897.

Zhang, Y., Mercier, J.L., Vergély, P., 1998. Extension in the graben systems around the Ordos (China), and its contribution to the extrusion tectonics of south China with respect to Gobi-Mongolia. Tectonophysics 285, 41-75.

Zhang, Y., Ma, Y., Yang, N., Shi, W., Dong, S., 2003. Cenozoic extensional stress evolution in North China. Journal of Geodynamics 36, 591-613.

~~Zhang, Z., Tyrrell, S., Li, C., Daly, S.J., Sun, X., Blowick, A., Lin, X., 2016. Provenance of detrital K-feldspar in Jianghan Basin sheds new light on the Pliocene-Pleistocene evolution of the Yangtze River. Geolocial Society of America Bulletin doi: 10.1130/b31445.1 http://gsabulletin.gsapubs.org/content/early/2016/04/27/B31445.1.abstract~~

~~Zhao, H., Li, S.H., 2002. Luminescence isochron dating: A new approach using different grain sizes. Radiation Protection Dosimetry 101, 333-338.~~

~~Zhao, Z., Wang, S., Jiang, F., Wu, X., Xiao, H., Tian, G., Liu, K., Yin, W., Xue, B.,~~

Formatted: English (United States)

~~Wang, S., 2002. Magnetostratigraphy and environmental records of laterite in Sanmenxia area. Marine Geology & Quaternary Geology 22, 93-97.~~

Zheng, H., Powell, C., Rea, D., Wang, J., Wang, P., 2004. Late Miocene and mid-Pliocene enhancement of the East Asian monsoon as viewed from land and sea. Global and Planetary Change 41, 147-155.

Zheng, H., Huang, X., Ji, J., Liu, R., Zeng, Q., Jiang, F., 2007. Ultra-high rates of loess sedimentation at Zhengzhou since Stage 7: Implication for the Yellow River erosion of the Sanmen Gorge. Geomorphology 85, 131-142.

Zheng, H., Clift, P., Wang, P., Tada, R., Jia, J., He, M., Jourdan, F., 2013. Pre-Miocene birth of the Yangtze River. PNAS 110, 7556-7561.

Zhu, H., Chen, K., Liu, K., He, S., 2008. A sequence stratigraphic model for reservoir sand-body distribution in the Lower Permian Shanxi Formation in the Ordos Basin, Northern China. Marine and Petroleum Geology 25, 731-743.

Zhu, R. X., Laj, C., Mazaud, A., 1994. The Matuyama-Brunhes and upper Jaramillo transitions recorded in a loess section at Weinan, north-central China. Earth and Planetary Science Letters. 125, 143-158.

Table Captions

Table 1. Fluvial terrace correlation between Sanmenxia and Kouma

~~Table 2. Optically stimulated luminescence dating~~

Figure Captions

Fig. 1. Map of the Fenwei graben and its surroundings, showing faults (from AFSOM, 1998), rivers, topography, and the locations of the four sub-basins (the Weihe, Lingbao, Yuncheng, and Fenhe basins). The locations of Figs 2 and 3 are also indicated. The inset map shows the major fault systems, plate motions, Bohai Gulf, and location within China.

Fig. 2. Maximum, mean, and minimum topography along a 50-km-wide swath along the Sanmen gorge (see Fig. 1 for location). Active faults and the interpreted long profile of the planation surface are also depicted (see also Fig. 4).

Fig. 3. Map of the study region showing topography (using the same data source as Fig. 1), active faults, and field locatities (see Fig. 1 for location).

Fig. 4. Field photos of the Sanmen gorge and its entrance. (A) View of the planation surface dominating the Xiaoshan along the Sanmen gorge, looking east from 34°51′09.36″ N, 111°19′34.16″E. (B) The westward dip of the planation surface (looking north from 34°46′03.27″ N, 111°17′53.48″E), the result of deformation close to the inlet of the Sanmen gorge. (C and D) Fluvial terrace staircase at Sanmenxia, looking west (C) and south (D). Five terraces have been identified below the planation surface, of which the uppermost (T5) is newly recognized. (E) Closeup view of the sedimentary sequence forming terrace T2 at Sanmenxia (see (D) for location). The fluvio-lacustrine Sanmen Formation, characterized by horizontally bedded mudstone, siltstone, clay, conglomerate, and sandstone, crops out below the terrace gravel.

Fig. 5. Transverse profiles through the fluvial terrace staircases at the field localities (Zhangbian, Sanmenxia, Dongcun, Xiaolangdi, and Kouma; see Fig. 3 for locations).

Note that the terrace staircases at Zhangbian, Sanmenxia and Dongcun are affected by normal faulting.

Fig. 6. Interpreted longitudinal profile of terrace levels along the Sanmen gorge, using height data from Table 1. The normal faults that define the ends of the gorge are depicted in Fig. 2 and 3.

Fig. 7. Magnetostratigraphy and pedostratigraphy of the aeolian deposits overlying the fluvial terraces and planation surface at Sanmenxia. These TL dates for T2 and interpreted chrons (black for normal geomagnetic polarity, white for reverse) for terraces T4, T3, and T2 are all from Pan et al. (2005a). For the newly recognized terrace T5 and the planation surface, paleomagnetic data from the overlying ~130-m- and 152-m-thick aeolian deposits are used to obtain age interpretations (of ~1.24 Ma and 3.63 Ma, respectively), using the Cande and Kent (1995) geomagnetic polarity timescale. However, these data are displayed here without filtering for noise. The magnetic susceptibility values are higher in the palaeosol units than those in the neighboring loess layers.

Fig. 8. A selection of the data from Fig. 7, illustrating the thermal demagnetization process used to identify the primary components of rock magnetization that indicate the polarity of the Earth's magnetic field at the time of deposition. For each figure part, the left-hand panel shows the horizontal (solid symbols) and vertical (open symbols) components of rock magnetization, whereas the right-hand panel shows how the strength of magnetization decreases with increasing temperature. (A) Sample PR-10.0 from the 10.0-m thickness of the aeolian section on the planation surface, a sample of Carbonate nodules. After a low-temperature overprint is removed, this sample is seen to be magnetized upward and southward, indicating reverse polarity. (B) Sample PR-0.5 from 0.5-m thickness of the aeolian section on the planation surface, a sample of Red Clay. After a low-temperature overprint is removed, this sample is seen to be magnetized downward and northward, indicating normal polarity. (C) Sample PL-69.0 from 69.0-m thickness of the aeolian section on the planation surface, a sample of loess. After a substantial overprint is removed, this sample is seen to be magnetized upward and southward, indicating reverse polarity. (D) Sample PL-109.0 from 109.0-m thickness of the aeolian section on the planation surface, a sample of loess.

This sample is seen to be magnetized downward and northward, indicating normal polarity. (E) Sample T5-33.0 from 33.0-m thickness of the loess section on terrace T5. This sample is seen to be magnetized downward and westward, indicating ambiguous polarity. (F) Sample T5-28.0 from 28.0-m thickness of the loess section on terrace T5. This sample is seen to be magnetized downward and northward, indicating normal polarity.

Fig. 9. Schematic diagram illustrating landscape evolution within the Fenwei graben. (A) The initial downfaulting, erosion, and filling of the Fenwei graben. (I) Development, in the Early Pliocene, of the graben as a result of extensional tectonism. (Π) Planation, circa 3.6 Ma (according to the magnetostratigraphic data), during infilling of the graben, marked by emplacement of the lower part of the Sanmen Formation. (B) Uplift and dissection of the planation surface after ~3.6 Ma. At this time the extension switched from the initial set of normal faults to a newer set in the hanging-walls of the initial set, resulting in narrowing of the graben. (C) Erosion, fill, and excavation of this narrower graben. (I) Erosion and fill when the narrower graben was occupied by an isolated fluvio-lacustrine system, during deposition of the upper part of the Sanmen Formation in the Early Pleistocene. (Π) Initial entrenchment of the Yellow River into the Sanmen Formation circa 1.2 Ma. At this time the former lake basin was disrupted and fluvial drainage first developed from west to east across the Xiaoshan, leading to the formation of the Sanmen gorge and incision into the Sanmen Formation. (D) Incision and terrace formation by the Yellow River at Sanmenxia since the late Early Pleistocene, creating the present fluvial terrace staircase.

Table 1

Table 1: Fluvial terrace correlation between Sanmenxia and Kouma

Site			Terrace 1		Terrace 2		Terrace 3		Terrace 4		Terrace 5		Planation surface
Name	Co-ordinates	H_o (m)	H (m)	h (m)	H (m)	h (m)	H (m)	h (m)	H (m)	h (m)	H (m)	h (m)	H (m)
Zhangbian	34°42′51″N, 111°01′13″E	307.0	317.0	1.0	NO	NO	338.0	3.0	381.7	1.0	395.4	0	520.0
Sanmenxia	34°48′06″N, 111°14′25″E	306.6	317.2	0	325.5	2.0	338.0	4.0	382.1	2.0	394.1	2.0	557.8
Dongcun	34°50′46″N, 111°34′07″E	249.5	261.9	0	270.3	3.9	300.5	2.3	325.0	0.6	427.0	0.4	647.0
Xiaolangdi	34°55′15″N, 112°23′58″E	133.8	142.3	3.1	NO	NO	193.5	3.9	229.9	3.6	291.7	5.8	381.4
Kouma	34°49′20″N, 112°46′18″E	89.8	99.8	0	NO	NO	115.0	0	NO	NO	145.0	0	200.0

For each site, H_o denotes the height of the Yellow River above sea level. For each river terrace and for the planation surface, H denotes height above sea level and h denotes the thickness of fluvial sediments (h=0 denoting sites where the terrace surface is cut into bedrock). NO denotes river terraces that are not observed at particular sites.

Figure 1

Click here to download high resolution image

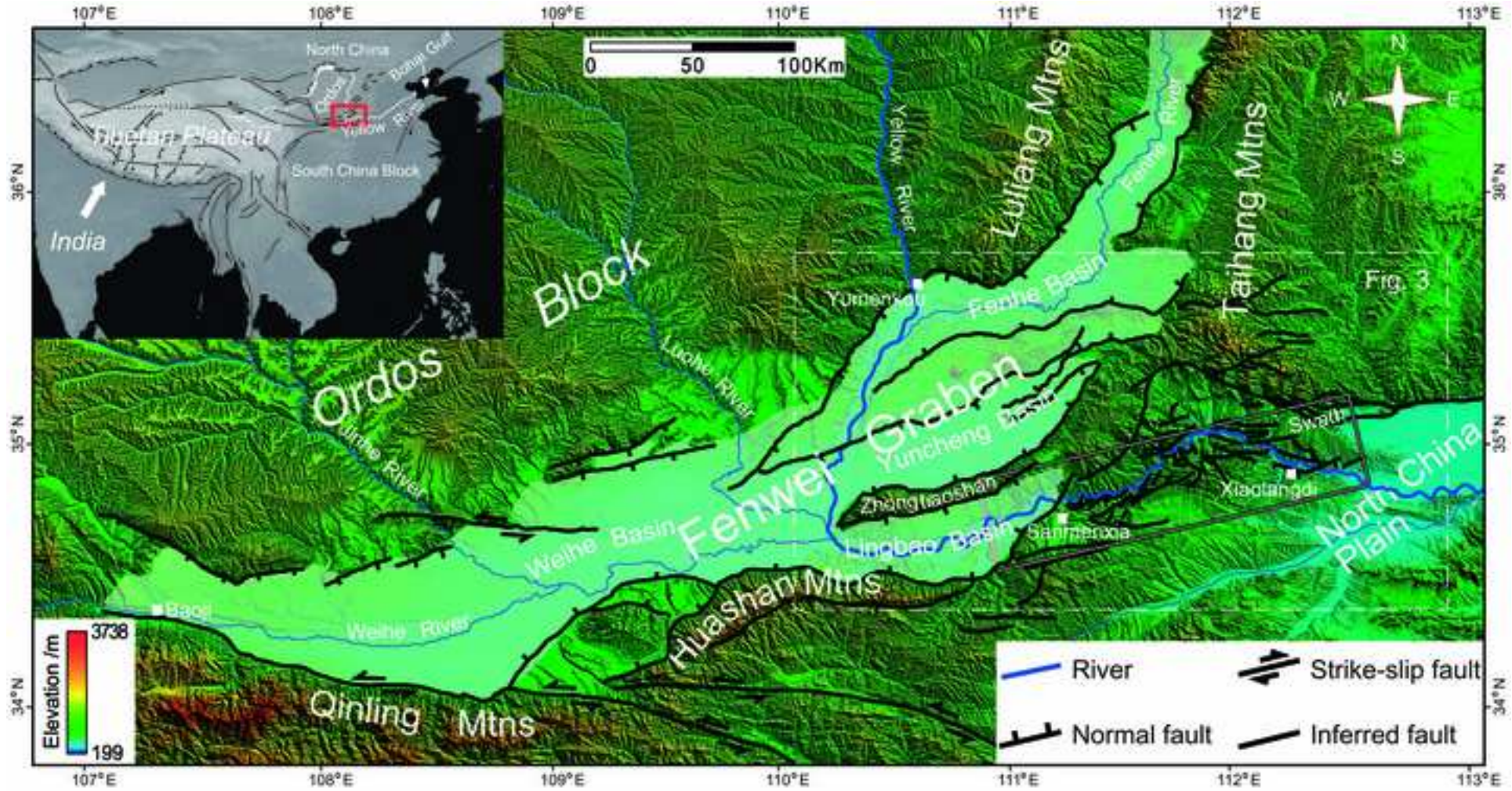

Figure 2

Click here to download high resolution image

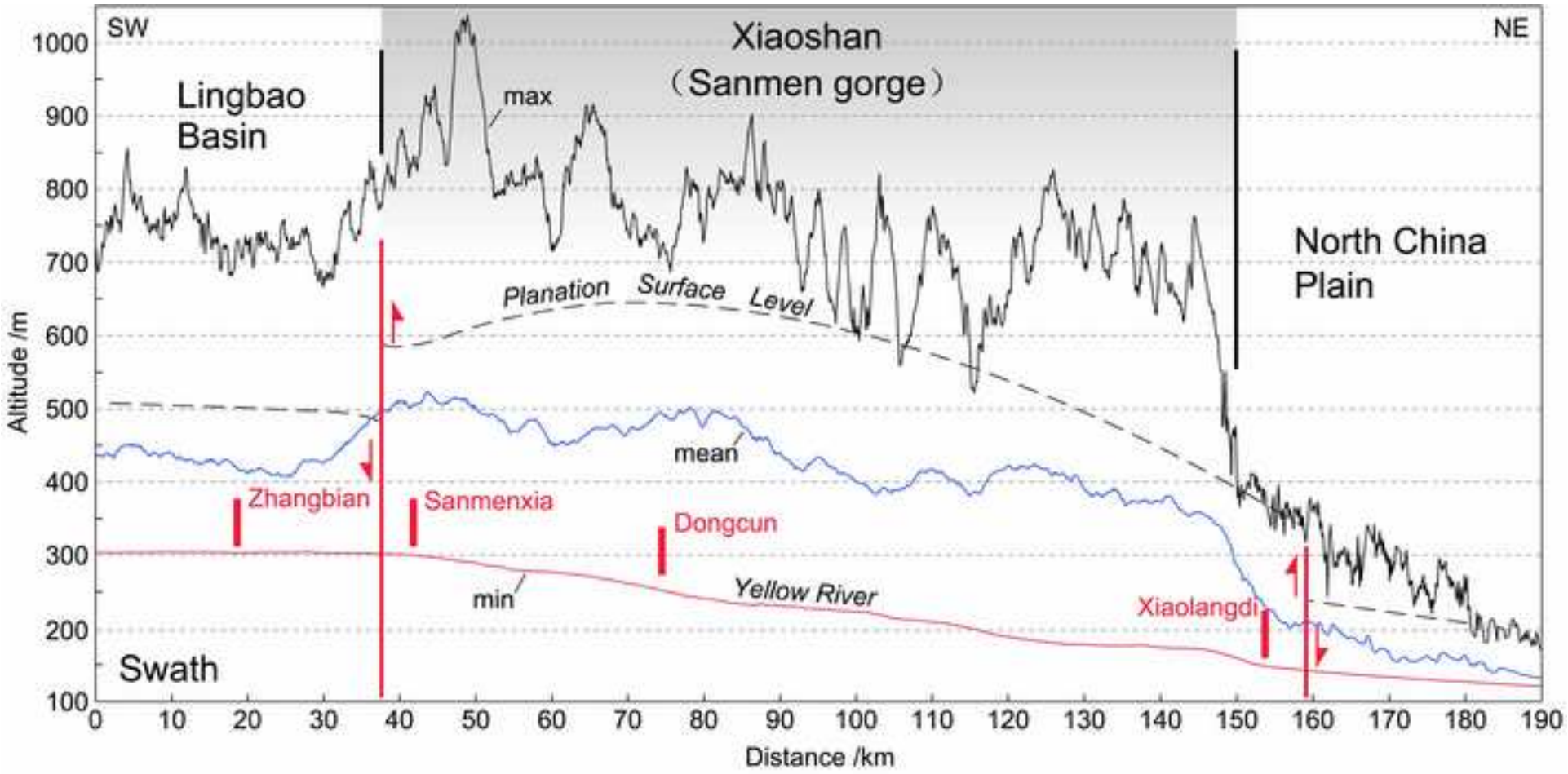

Figure 3

Click here to download high resolution image

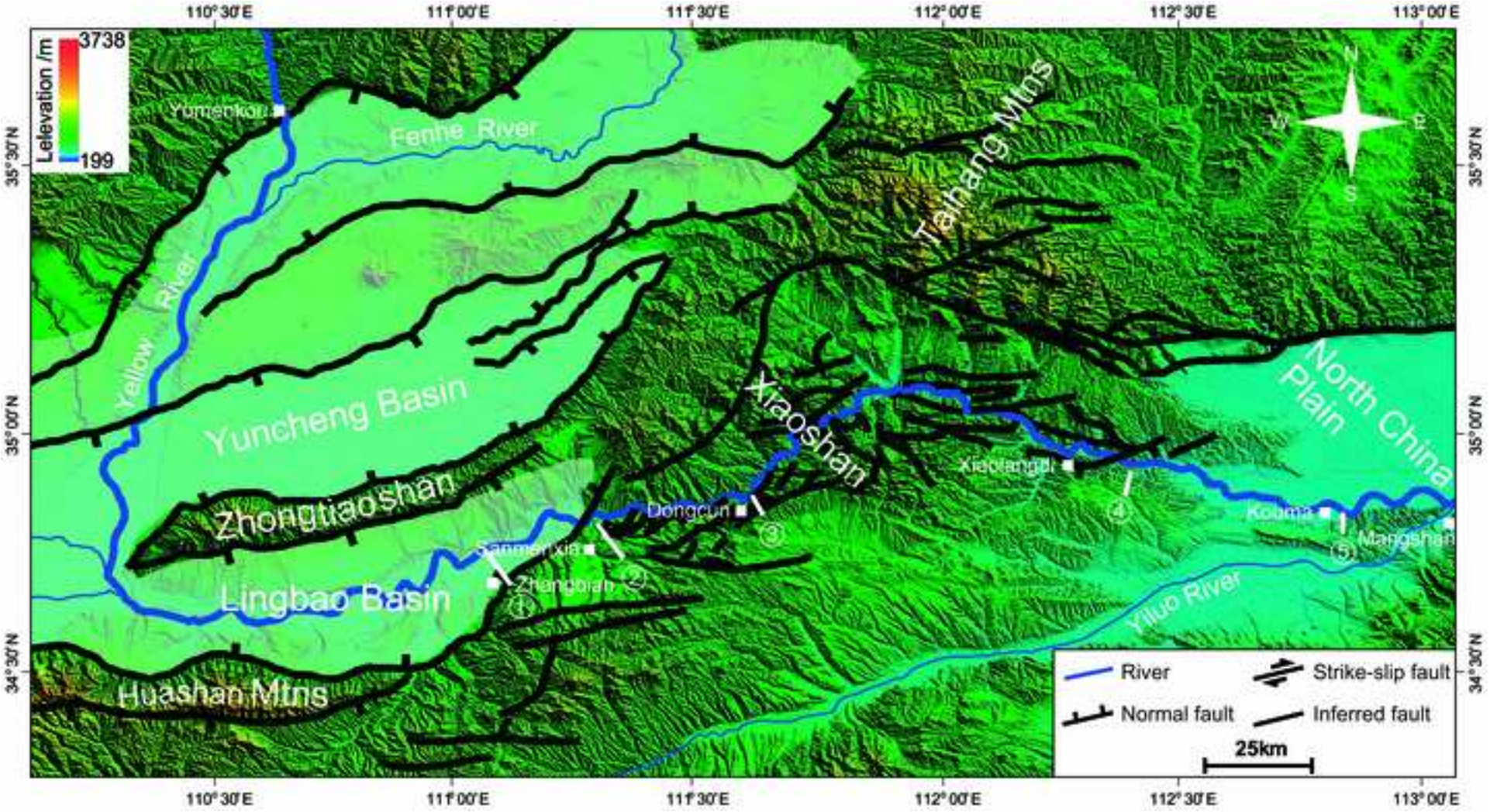

Figure 4

Click here to download high resolution image

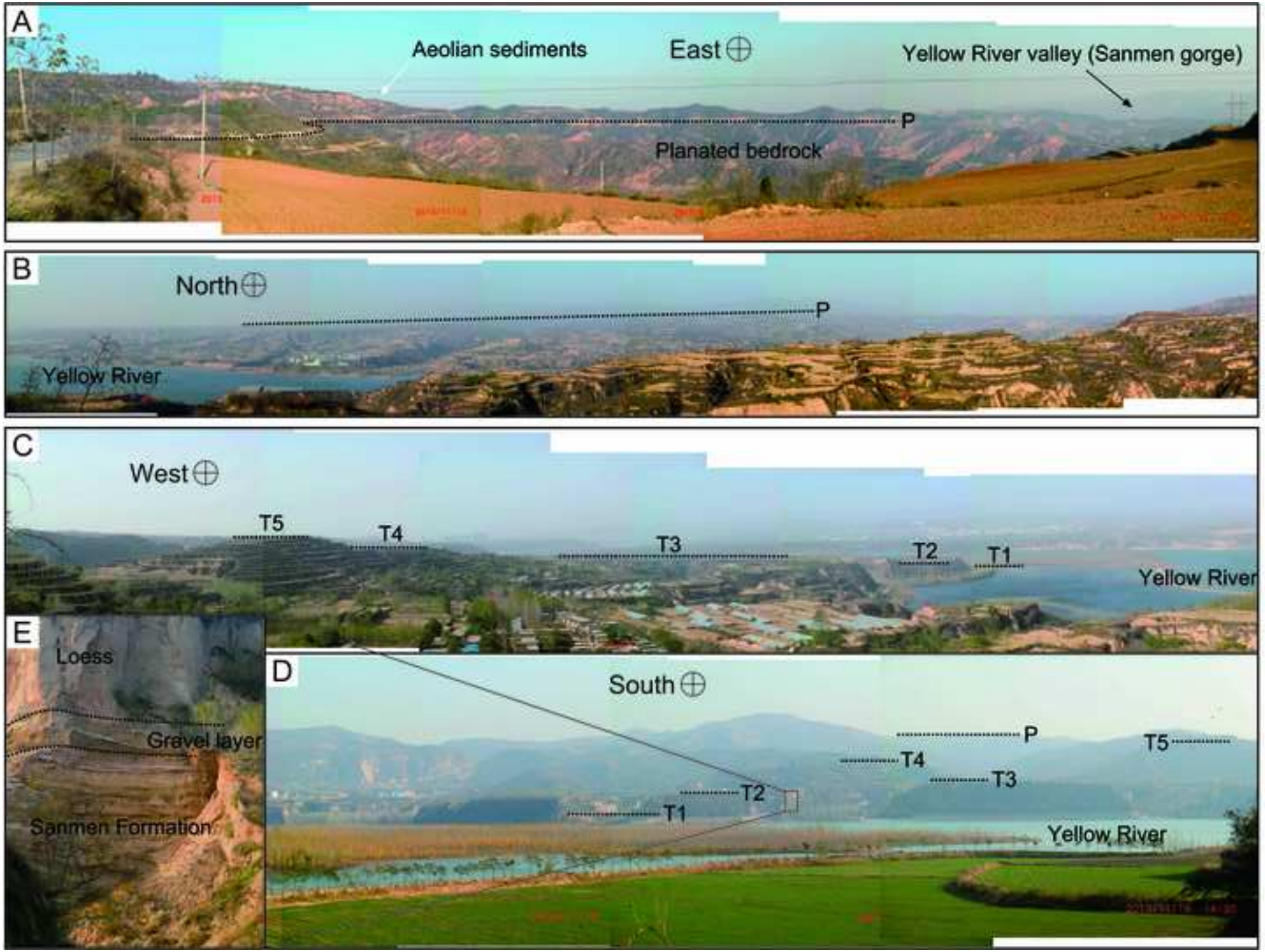

Figure 5

Click here to download high resolution image

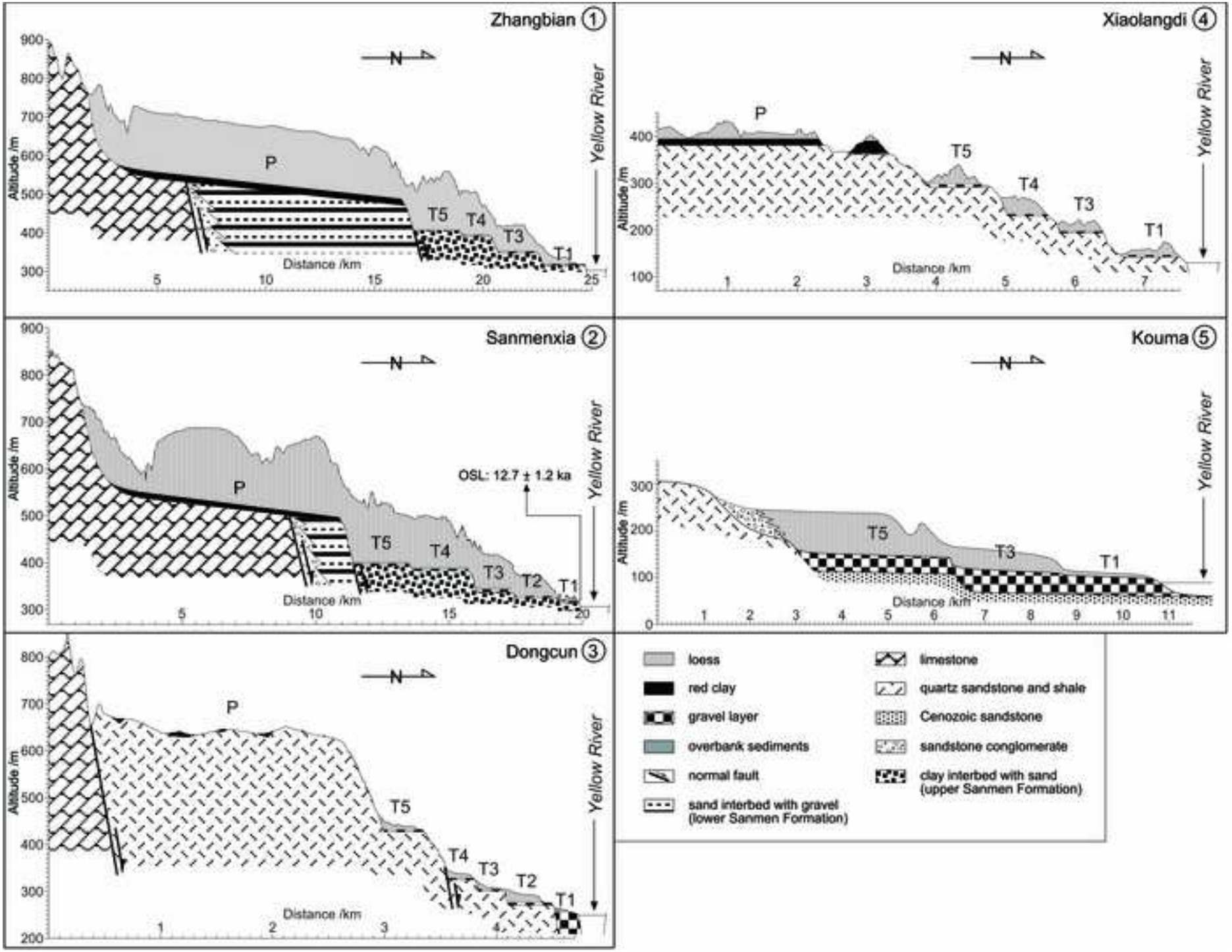

Figure 6

Click here to download high resolution image

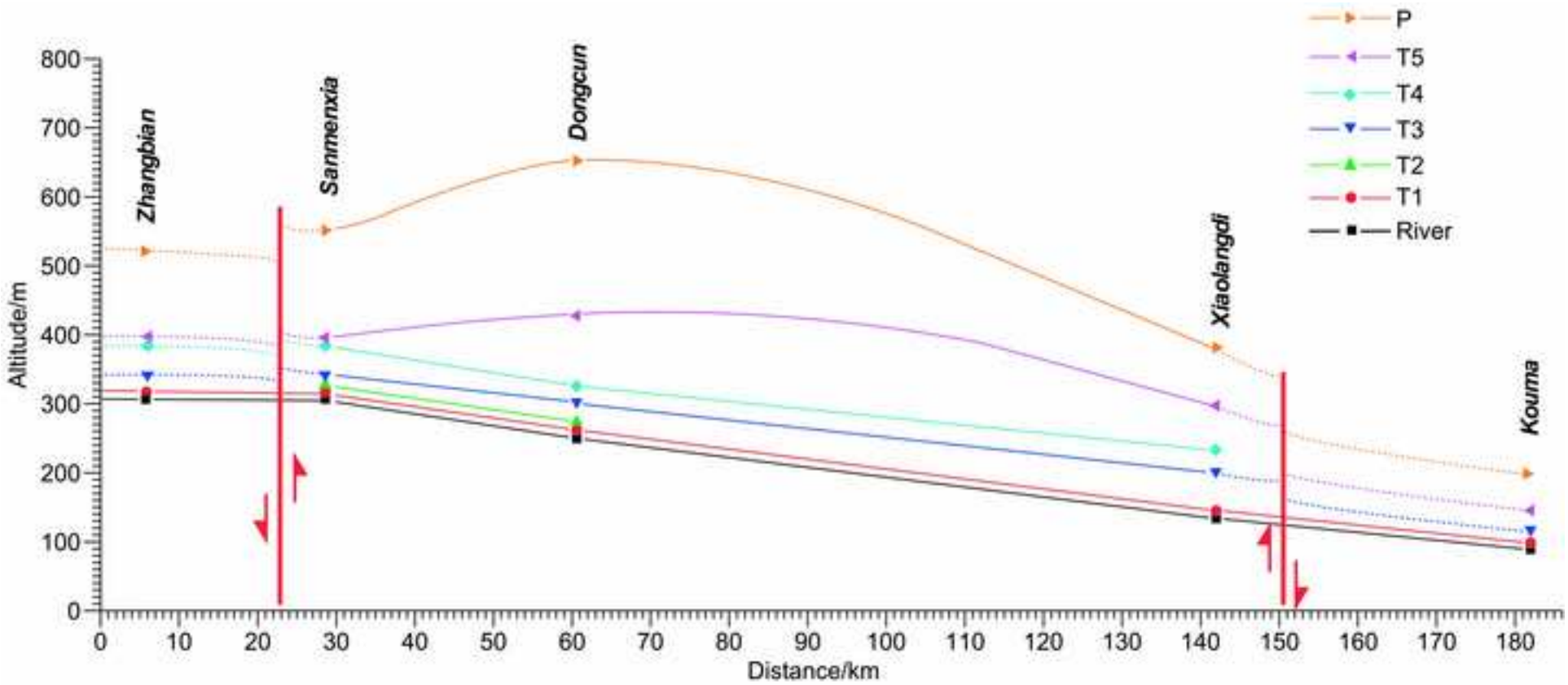

Figure 7

Click here to download high resolution image

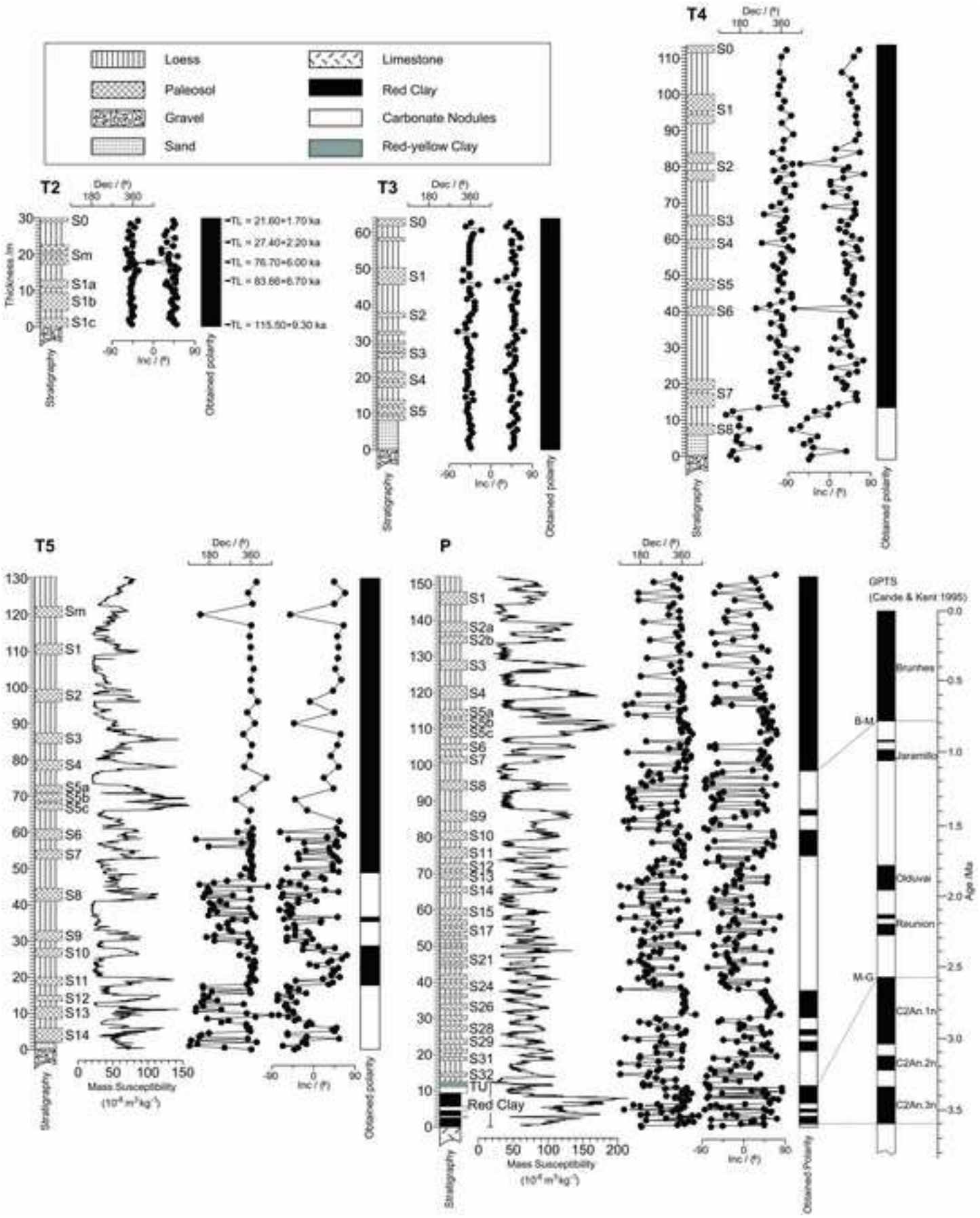

Figure 8

Click here to download high resolution image

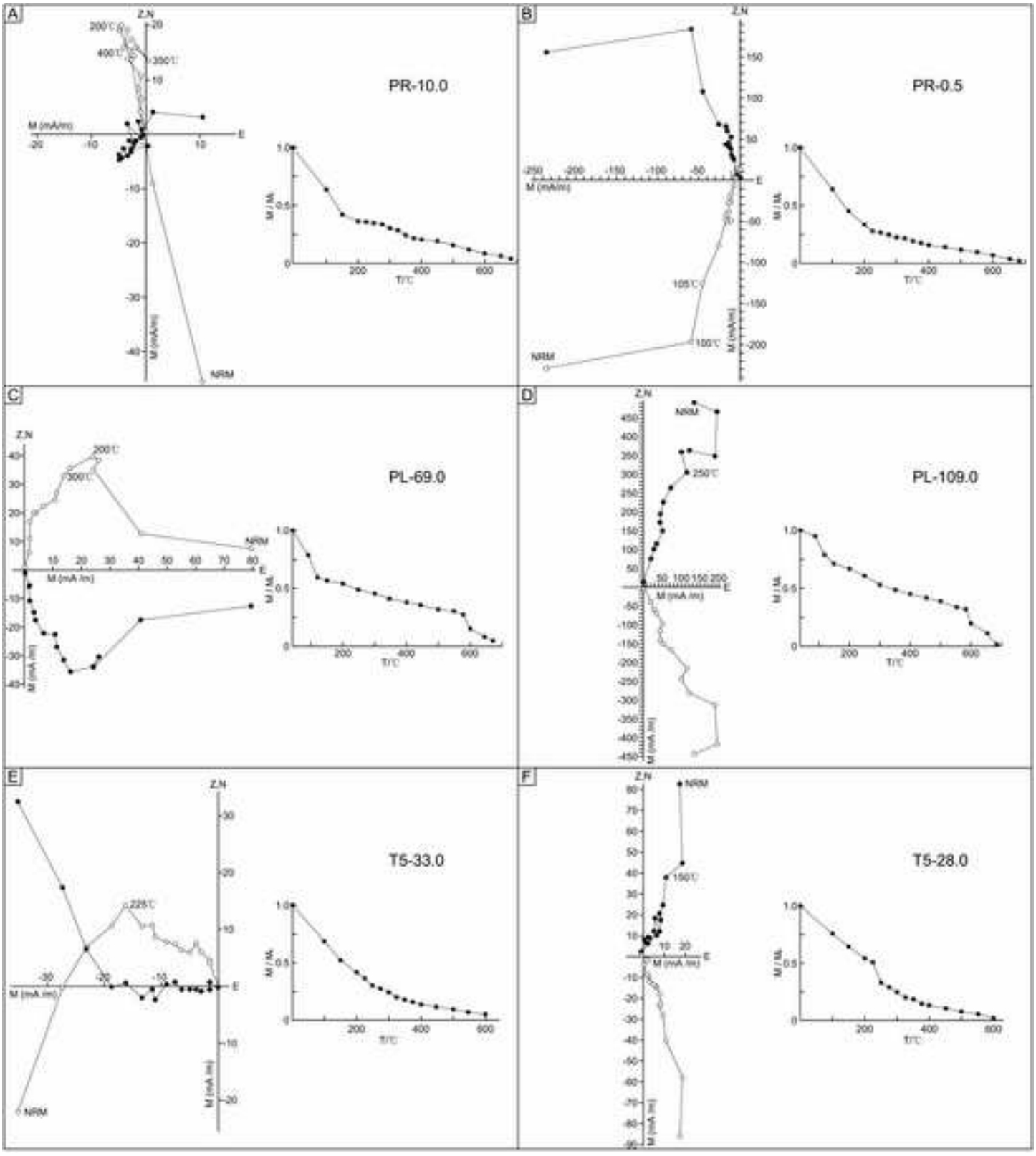

Figure 9

Click here to download high resolution image

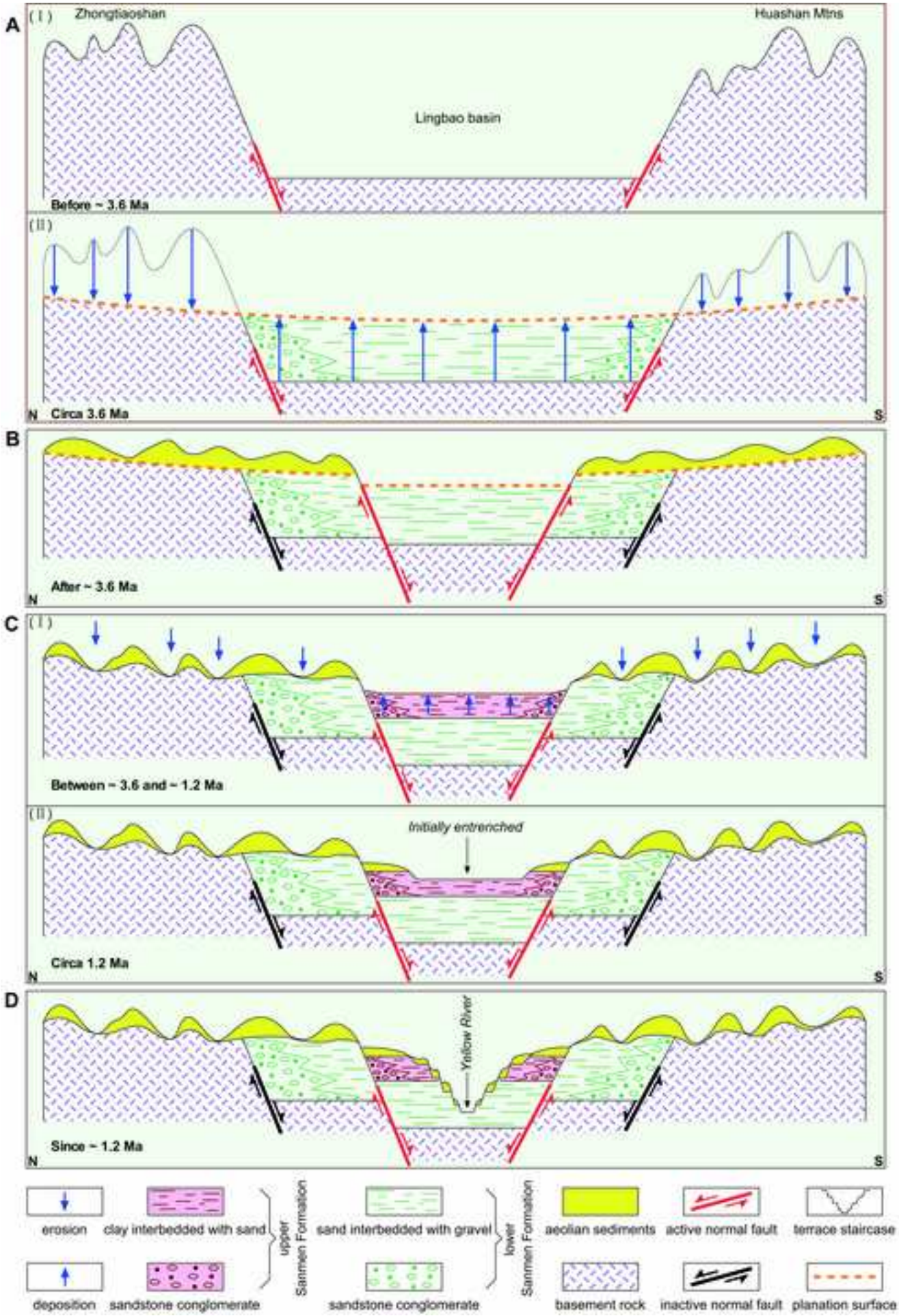

Research Highlights

- We reconstructed a 3.6 Ma sequence based on the planation surface and terraces along the Sanmen gorge.
- The landscape evolution from basin filling to excavation was outlined under the constraint of this chronology.
- The present-day Sanmen gorge was formed by westward capturing the paleolake within the Fenwei graben.
- Gorge formation may have been initiated by lake overflow during the period 3.63–1.24 Ma.
- The dramatic increase in deposition rates in the Bohai Gulf resulted from the establishment of an integral Yellow River catchment.

***Response to Reviewers**

Dear authors,
I reviewed the re-revised version of your manuscript submitted as part of the FLAG special issue in QSR. Despite some improvements, the key issues raised in my last review remain :
-concerning the structure : the « methods » section still include data, especially in section 2.2. Similarly some essential information which should appear early in the manuscript is only exposed in the discussion. This especially concerns the existing age control (lines)
-actually, the state of the art related to the previous geochronological interpretation (your section 1.4, which should also include section 1.5 since both deal with the same topic) must be improved, especially 1) by including all the chronological evidences, 2) by underlining the unconsistencies, and 3) by explaining that your aim is to try to provide a more consistent reconstruction. Otherwise we are left with the feeling that this paper does not bring new information !! So I strongly advice you to rewrite carefully this section, which is according to me one of the most important of the manuscript.

- We are grateful to the referee for valuable comments and constructive suggestions. The structure of this manuscript has been revised completely following the comments by the reviewer. The section mentioned by the referee has been rewrite to make a good expression.

-the text is at several places redundant (this is underlined by your use of « see below », or « abovementioned »), and this makes it more confusing. Please check the ms to remove all useless repetitions. I also advice you not to develop too much some parts that does not directly relate to the aim of your study, for example the OSL dating of the youngest terraces does not appears to be really significant…

- Reply: Yes according to the comment by the reviewer, our manuscript has been reconstructed and these useless repetitions has also been removed. Now it seems to be compendious and clear.

- despite not being native speaker I think a check of the language is really necessary ! this could be easily done by some of the co-authors

- Reply: As co-authors of our manuscript, Prof. David Bridgland and Jef Vandenberghe have done this work.

Some more specific comments (but to be considered as well) :
-sctions 1.1 and 1.2 to be merged : actually it is difficult to deal with the significance of fluvial archives without having provided a general overview of the morphostructural context.
-the hiatus between the ⩾1.24 Ma age for the gorge formation and the 1 Ma age for the deposition must be explained in a less allusive way than done in the cover letter and lines
Actually 250 ka is quite a long time…And if you want to explain this by dating uncertainty, please provide all uncertainties throughout the manuscript (I strongly advice you to do so)

- Reply: The paleomagnetic dating does not provide a exact uncertainty, despite a statistical error within this method. This inaccuracy can reach 240 ka in comparison with a long time

scale of 1 Ma. In addition, we have no data to discuss the chronological discrepancy. Therefore, we have added a symbol of ‘circa’ at the front of the age to express a approximate relationship.

-l.120 vs l.131 : crescent of S shaped ?

- Reply: This has been revised into ‘crescent-shape’.

-l.177 : please rephrase beginning of section.

- Reply: Yes, it has been revised.

-l.181-185 : sentence not clear

- Reply: It has been removed.

-l.192 : length of the Yellow river to be provided earlier

- Reply: The construct of this manuscript has been revised. here is suitable to provide the information of the Yellow River.

-l.210 : distribution of sediments : too allusive
-sections 1.4 and 1.5 to be merged (see above)

- Reply: It has been removed. The sections 1.4 and 1.5 have been modified according to the referee’s comment.

-l.250 : incomplete age control : too allusive

- Reply: Yes, this should be attributed to incomplete age control, because previous work by Pan et al. (2005a) did not find the uppermost terrace.

-l.283 : these -> the
-section 2.2 to be placed elsewhere, it is not methods

- Reply: They has been revised based on the suggestion of this referee.

-l.315-316 : please be consistent to use either ka or Ma…

- Reply: It has been revised.

-l.323 : aid correlation : how ?

- Reply: Based on the pattern of magnetic susceptibility.

-l.357 : formation age

- Reply: It was removed.

-l.381 : it would be helpful to have the Loess plateau located on a map…

- Reply: The object of this paper is not concerned with the distribution of the loess within China. Anyone who want to know about the information of the Chinese loess plateau can go to the reference of Liu (1985). This literature has been listed in the reference of our paper. In addition, so much information was superposed on the map, providing the extent of the loess plateau will make a confused expression.

-l.414-413 : not clear

- Reply: This is a clear expression. The loess stratigraphy can be correlated on the basis of the magnetic susceptibility pattern.

-l.419-426 : better focus on the Red clau before the loess as they are older ?

- Reply: This is just a description of magnetic susceptibility pattern in the result section.

-l.433-434 too allusive, remove or explain.

- Reply: It has been removed.

-section 3.3 : please to not mix depths and elevation above reference levels (eg l.456/463)

- Reply: We never mix, this is thickness.

-l.482 : cm/ky

- Reply: It has revised.

-l.502/504 : T5 is not new if it has been recognized earlier…

- Reply: In comparison with the work by Pan et al. (2005a), the terrace T5 is newly recognized. Although, this terrace may be identified by Kong et al. (2014), the age determination is not successful. Therefore, our paper still define T5 as a newly recognized terrace.

-l.517 : height above river : is it reliable ? please discuss this to justify your choice.

- Reply: Fluvial terrace is the remnant of previous river bed. If the terrace is not affected by tectonic activity, the same terrace maybe have a approximate height above river. Therefore

the height of one terrace above river bed is a important evidence for terrace correlation. Taking account of the height error, we have to say ‘tentative correlation’.

-l.566-567 please provide evidences

- Reply: The evidence for the continuous aeolian deposition in the present study region has been provided early in this manuscript.

-l.622 : reference to Molnar too allusive.

- Reply: No, we have described our result early, and then made a comparison with Molnar (2004).

-l.639-644 too allusive

- Reply: No, we have made a clear expression.

l.650 and after : this does not look a very original conclusion, bette remove this section…

- Reply: Removed.

-l.672 : some of the ages you indicate do not derive from your research !

- Reply: Providing a complete chronological framework for the terrace sequence is helpful for readers.

I hope you'll be able to take this comments into consideration (and especially the main ones exposed at the beginning of this review), to prepare the definitive version of the manuscript. best wishes, Stéphane Cordier

Dear Cordier, many thanks for your help. We have got much suggestion and help for David and Jef. Based on their revision and suggestion, I have made a thorough modification to the construct of this manuscript.